T.R.
BOLU ABANT İZZET BAYSAL UNIVERSITY
INSTITUTE OF GRADUATE STUDIES
Department of Physics

INVESTIGATION OF NEUTRAL TRIPLE GAUGE COUPLING VIA $pp \rightarrow ZZ$ PRODUCTION WITH ANOMALOUS COUPLING APPROACH FOR FUTURE HADRON COLLIDERS

MASTER OF SCIENCE

SHAHAD AHMED AL-YOUSİF

ACADEMIC SUPERVISOR
Prof. Dr. Abdulkadir ŞENOL
ACADEMIC CO-SUPERVIZOR
Prof. Dr. Haluk DENİZLİ

BOLU, KASIM - 2022

APPROVAL OF THE THESIS

INVESTIGATION OF NEUTRAL TRIPLE GAUGE COUPLING VIA $pp \rightarrow ZZ$ PRODUCTION WITH ANOMALOUS COUPLING APPROACH FOR FUTURE HADRON COLLIDERS submitted by **Shahad AHMED AL YOUSIF** and defended before the Examining Committe Members listed below in partial fulfillment of the requirements for the degree of **Master of Science** in **Department of Physics, Institute of Graduate Studies of Bolu Abant Izzet Baysal University in 16.11.2022** by

Examining Committee Members	**Signature**
Supervisor Prof. Dr. Abdulkadir ŞENOL Bolu Abant Izzet Baysal University	....
Member Prof. Dr. İlkay TÜRK ÇAKIR Ankara University	....
Member Assoc. Prof. Dr. Ali YILMAZ Bolu Abant Izzet Baysal University	....

Prof. Dr. İbrahim KÜRTÜL
Director of Instıtute of Graduate Studies

ETHICAL DECLARATION

In this thesis dissertation that was properly prepared according to the Thesis Writing Rules of Bolu Abant İzzet Baysal University of the Institute of Graduates Studies, I hereby declare that;

- All data, information, and documents presented in the thesis were obtained in accordance with the academic and ethical rules,
- All data, documents, assessments, and results were presented in accordance with the scientific ethical and moral rules,
- All works that were benefitted in the thesis were appropriately cited,
- No alteration was made in the data used,
- Study presented in this thesis is original,

Otherwise, I declare that I accept the loss of all my rights in case any contradiction that may arise against me.

Based on the plagiarism report that was generated on the date of 17/11/2022 by using predetermined filtrations set by Directorate of Institute of Graduate Studies of the Turnitin programme, a plagiarism detection sofware, the similarity index detected was 30 %.

Shahad AHMED AL-YOUSİF

ABSTRACT

INVESTIGATION OF NEUTRAL TRIPLE GAUGE COUPLING VIA
$pp \rightarrow ZZ$ PRODUCTION WITH ANOMALOUS COUPLING APPROACH
FOR FUTURE HADRON COLLIDERS
MSC THESIS
SHAHAD AHMED AL YOUSIF
BOLU ABANT IZZET BAYSAL UNIVERSITY
INSTITUTE OF GRADUATE STUDIES
DEPARTMENT OF PHYSICS
(SUPERVISOR: PROF. DR. ABDULKADIR SENOL)
(CO-SUPERVISOR: PROF. DR. HALUK DENIZLI
BOLU, NOVEMBER 2022
xiv + 52 pages

Examining the self-couplings of Electroweak gauge bosons as determined by the non-Abelian gauge nature of the Standard Model (SM) provides an important opportunity for the validity of the SM and the existence of new physics beyond the SM to the high energy scale. The sensitivity of anomalous ZZZ and ZZγ vertex couplings ($f_4^{\gamma,Z}, f_5^{\gamma,Z}$) defined in the anomalous coupling approach is investigated for various future circular hadron collider options, namely HL-LHC ($\sqrt{s} = 14\,TeV, \text{Lint} = 3\text{ a}b^{-1}$), HE-LHC ($\sqrt{s} = 27\text{ TeV}, \text{Lint} = 5\text{ a}b^{-1}$), FCC-hh ($\sqrt{s} = 100\text{ TeV}, \text{Lint} = 30\text{ a}b^{-1}$) via pp ⟶ ZZ production with different decay channels of the Z boson. The signal and background events are generated with CalcHEP package program. The resulting events are passed through PYTHIA for hadron shower and Delphes for detector effects, and the kinematic distributions of the final state particles are obtained for the different decay channels of the Z boson. Sensitivities on the anomalous triple gauge couplings are We calculated with 95% confidence level via χ^2 test with the corresponding integrated luminosities of future hadron colliders for different decay channels of Z boson.

KEYWORDS: Anomalous triple gauge couplings, Future hadron colliders, ZZ production.

ÖZET

GELECEKTEKİ HADRON ÇARPIŞTIRICILARI İÇİN ANORMAL KUPLAJ YAKLAŞIMIYLA $pp \rightarrow ZZ$ ÜRETİMİ YOLUYLA YÜKSÜZ ÜÇLÜ AYAR KUPLAJLARININ İNCELENMESİ

YÜKSEK LİSANS TEZİ

SHAHAD AHMED AL YOUSIF
BOLU ABANT İZZET BAYSAL ÜNİVERSİTESİ
LİSANSÜSTÜ EĞİTİM ENSTİTÜSÜ
FİZİK ANABİLİM DALI

(TEZ DANIŞMANI: PROF. DR. ABDULKADIR ŞENOL)
(İKİNCİ DANIŞMAN: PROF. DR. HALUK DENİZLİ)

BOLU, KASIM - 2022
xiv + 52 sayfa

Standart Modelin (SM) Abelian olmayan ayar doğası tarafından belirlenen Elektrozayıf ayar bozonlarının kendi kendine eşleşmelerini incelemek, SM'nin geçerliliği ve SM'nin ötesinde yüksek enerji ölçeğine yeni fiziğin varlığı için önemli bir fırsat sağlar. Anormal eşleşme yaklaşımında tanımlanan anormal ZZZ ve ZZγ köşe kuplajlarını(($f_4^{\gamma,Z}, f_5^{\gamma,Z}$) hassasiyeti, Z bozonunun farklı bozunum kanalları ile pp ⟶ ZZ üretimi yoluyla HL-LHC ($\sqrt{s} = 14\, TeV$, Lint $= 3$ ab^{-1}), HE-LHC ($\sqrt{s} = 27$ TeV, Lint $= 5$ ab^{-1}), FCC-hh ($\sqrt{s} = 100\, TeV$, Lint $= 30$ ab^{-1}) gibi çeşitli dairesel hadron çarpıştırıcı seçenekleri için araştırılmıştır. Sinyal ve arka plan olayları CalcHEP paket programı ile üretilmiş. Elde edilen olaylar hadron duşu için PYTHIA'dan ve dedektör etkileri için Delphes'den geçirilmişve Z bozonunun farklı bozunma kanalları için son durum parçacıklarının kinematik dağılımları elde edilmiştir. Anormal üçlü ayar bağlantılarındaki hassasiyetler, Z bozonunun farklı bozunma kanalları için gelecekteki hadron çarpıştırıcılarının karşılık gelen entegre parlaklıkları ile χ^2 testi yoluyla % 95 güvenilirlik seviyesiyle hesaplandı.

ANAHTAR KELİMELER: Anormal üçlü ayar bağlaşımları, Gelecek hadron çarpıştırıcıları, ZZ üretimi.

TABLE OF CONTENTS

LISTE OF FIGURE

Page

LIST OF TABLES

LIST OF PICTURES

Page

LIST OF ABBREVIATIONS AND SYMBOLS

ATLAS	: A Toroidal LHC Apparatus
BR	: Branching Ratio
BSM	: Beyond Standard Model
CERN	: Conseil European pour la recherche
CalcHEP	: Calculator for High Energy Physics
CPC	: CP-conserving
CPV	: CP-Violation
EFT	: Effective Field Theory
EW	: Electro-Weak
FCC	: Future Circular collider
HE-LHC	: High Energy Large Hadron Collider
HL-LHC	: High Luminosity Large Hadron Collider
LHC	: Large Hadron Collider
MC	: Monte Carlo
Pb	: Pico barn
SM	: Standard Model
TeV	: Tera-Electron Volts
TGC	: Triple gauge coupling
$\boldsymbol{p_T}$	: Transverse Momentum.
$\boldsymbol{\eta}$	: Pseudo Rapidity
ET	: Missing Transverse Energy
$\boldsymbol{\mathcal{L}}$	: Lagrangian
χ^2	: Chi Square
$\sqrt{\boldsymbol{s}}$	: Center of mass energy

ACKNOWLEDGEMENTS

My greatest appreciation is to Prof. Dr. Abdulkadir Şenol for his superior guidance and his patience throughout the whole process. I felt very confident in my steps, knowing he is close by to assist me accomplishing this mission. It was an excellent experience and a great scientific adventure for me. It did transform me into a better student of science and a good teacher in the future. I always be indebted to him.

I want also to thank Prof. Dr. Haluk Denizli for his kindness and support.

I also would like to acknowledge the support I got from the members and staff of the University of Bolu Abant İzzet Baysal.
I also thank my family who stood by me the whole entire way and who believed in me and didn’t rest until I achieve what I distend to achieve.

I also thank my new family, a husband and a new baby who encouraged me to get the highest degree in my education.

Finally, I thank those people who were very kind and generous with me.

1. INTRODUCTION

The pair production of gauge bosons at hadron colliders can shed light on the electroweak sector of the Standard Model (SM). Not only this, but it can be of great importance in searching for new physics beyond the SM (1,2). In particular, the pair production of Z bosons is one of the important processes in the search for neutral triple gauge boson couplings which vanish in the SM at tree-level.

Future hadron colliders will offer the possibility to test both the SM and its extensions at high energies and/or high luminosities (3, 4). This can be done through analyzing the collected data from the collisions aiming to find resonances of new particles for example in mass spectra (4). Another possibility to do that, is to probe the couplings between particles that are forbidden in the SM at tree-level.

In the SM, couplings such as ZZZ, do not exist at tree-level. However, these couplings can emerge in some extensions of the SM and hence it is possible to search for their signatures at colliders. This search will be significantly supported by the increase in the center of mass energy in planned future hadron colliders and also from the increase in integrated luminosities.

This thesis is organized as follows: in chapter 1, we give a brief introduction to the SM, the electroweak interactions, triple Gauge Couplings (TGCs) and the missing parts in the SM. In chapter 2, highlight some directions for Beyond Standard Model (BSM) physics and discuss the approach used in carrying out the investigation in this thesis namely, the anomalous couplings approach. In chapter 3, we give the relevant details of the future hadron colliders HL-LHC, HE-LHC and FCC-hh where the processes under investigation in this thesis will be explored. Chapter 4 is devoted for presenting the aim and scope of the study in this study. In chapter 5 we display the method used in performing the required calculations. In addition, in that chapter also, we show our results for the processes under concern namely, $pp \rightarrow ZZ \rightarrow ll\nu\nu, pp \rightarrow ZZ \rightarrow qq\nu\nu$, $qq \rightarrow ZZ \rightarrow llqq$ and $pp \rightarrow ZZ \rightarrow l^+l^-l^+l^-$ at a particular set of colliders including FCC-hh, HE-LHC and HL-LHC using anomalous couplings approach. These results include the cross sections, the kinematic distributions of specified particles in the final states and the sensitivities. Finally, in chapter 6, we present our conclusions. Historical Background of Standard Model.

1.1 Historical Background of Standard Model

The Standard Model (SM) describe to a great content the nature at the subatomic level. SM is a quantum field theory that has been tested for decades. It has been proven to be in agreement with most of the observation up to date. In the context of the quantum field theory, each particle can be described by one field. This is also true for the force carriers including gluons, photons, gluons, $W^{\pm}$ and Z bosons. The SM is the theory that describes three of the four known mean forces governing our universe namely, the electromagnetic, weak, and strong forces. In addition, SM accounts for the interactions of subatomic particles with these forces (5).

The SM was formulated in the second half of the 20th century, through the pioneering work of three scientists. With the current formulation being finalized in the mid-1970s upon experimental confirmations of the existence of heavier quarks, then the top quark (1995), the tau neutrino (2000), and finally the discovery of the Higgs boson (2012). Moreover the SM predicted, with an impressive accuracy, different properties of the weak neutral currents as well as the presence of W and Z bosons with masses equal their measured ones(5).

The SM is a gauge theory that was inspired by the work of many physicists working in both theoretical and experimental fields.

In the year 1954, Yang and Mills showed that the strong interaction can be described by non-abelian gauge group (6). This proposal can be considered as extending the concept of the abelian gauge group describing the quantum electrodynamics to account for strong and weak interactions. In the year 1957, parity violation was observed in the weak interaction. Four years later, Sheldon Glashow formulated a theory for unification of the weak and electromagnetic interactions. Few years later, a novel mechanism, known after that as the Higgs mechanism, was introduced to explain how quarks, charged leptons and the W and Z bosons acquire their masses. The Higgs mechanism was then incorporated into Glashow's electroweak interaction by Weinberg and Abdus Salam in 1967. This leads to the familiar form of the SM currently we know (7).

The electroweak theory predictions were supported by the discovery of the neutral currents resulting from the exchange of Z boson at CERN in the year 1973. As a result of this success, Glashow, Weinberg, and Salam won Nobel Prize in Physics in 1979 for their role in formulation of the SM. In the years followed that, lot of SM predictions were confirmed to be true. For instances, in 1983, the weak gauge bosons Z and W were observed with a ratio of masses in agreement with the SM prediction (7).

The theory describing the strong interaction is known as Quantum Chromodynamics (QCD). It was formulated in 1973–1974 upon the discovery of the asymptotic freedom which attracts more researches to QCD (8,9,10).

Triman and Pais in 1975 (11) introduced the concept "Standard Model" firstly to refer to the electroweak theory having 4 quarks known at that time (12). Contrary to that, Weinberg stated that he invented the SM term, and utilized it when he gave a talk in France in 1973. The SM particle sector contains twelve spin 1⁄2 fermions.

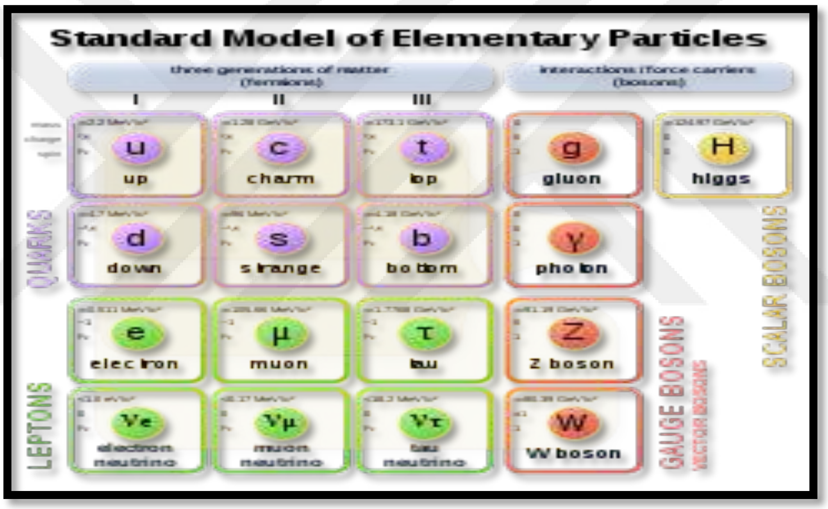

Figure 1.1. Standard Model of particle physics (13).

Fermion

A particle obeying Fermi–Dirac statistics is called fermion. In general, fermion has half odd integer spin. Fermions must respect the Pauli Exclusion Principle. They include all quarks and leptons, as well as all composite particles made of an odd number of these, such as all baryons which consist of 3 quarks or antiquarks. Fermions are totally different than bosons, which respect Bose–Einstein statistics (14). Some fermions do not have internal structure, such as leptons and quarks, while other fermions are composed of other particles, such as the proton which is composed of three quarks. Fermions additionally have another specific property: their decays must conserve baryon or lepton quantum numbers.

The Paul Exclusion Principle implies that, in a giving time only one fermion can exist in a given quantum state at a given time. This is not the case for bosons which generally act as the force carrier mediating the main interactions. Fermions display superfluity for uncharged particles while they show superconductivity for charged particles both happens at low temperatures. It’s well known that the essential building blocks of everyday matter are composed of fermions. Paul Dirac came up with the name fermion which was the surname of the famous scientist Enrico Fermi (15).

Bosons

A boson refers to a particle that obeys a kind of statistics known as Bose–Einstein statistics. It has a spin that must be an integer number such as 0, 1,2, etc.…. The name boson was given by Paul Dirac to honor Satyendra Nath Bose, an Indian physicist and professor of physics at University of Calcutta and at University of Dhaka for his significant impact on developing, together with Albert Einstein, the Bose–Einstein statistics, which established a theoretical framework of the properties of elementary particles (16).

Among the known bosons one can refer to photons, gluons, W and Z bosons, and the mot recently discovered Higgs boson (16). Some composite particles such as mesons are also bosons. A consequence of respecting the Bose–Einstein statistics, there is no restriction on the number of bosons occupying the same quantum state. Gauge bosons are the force mediators of the main forces governing our universe (17). A Bose–Einstein condensate occurs as a result of cooling down a gas of Bose particles to very low temperatures close to the absolute zero temperature. Consequently, the kinetic energy of the particles approaches to an almost negligible value. Then, the particles condense into states with minimum energy. This explains the phenomena of the superfluity (17). In Figure 1.2, we show a schematic graph of a classification of elementary particles into fermions, bosons and hadrons.

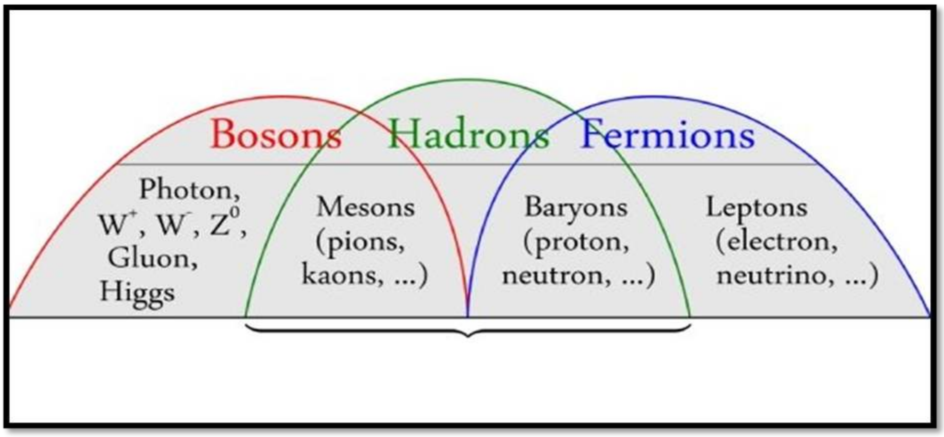

Figure 1.2. Schematic representation of a classification of elementary particles into fermions, bosons, and hadrons (17).

1.2 Electroweak Interactions

Particle decays can be achieved through the weak interactions. For particles to undergo the weak and electromagnetic interactions, the condition of the presence of the electric and color charges respectively must hold. Satisfying this condition is not guarantee for all SM particles and thus not all of them can interact with both interactions. On the other hand, this is not the case regarding the weak interactions, introduced by Fermi to explain the beta decay, where all SM particles undergo the weak interaction (18). In the Fermi theory, weak interaction was considered as contact charged current interactions having the same current-current structure in a similar way to the electromagnetic interactions. The weak and electromagnetic interactions were thought to be completely two different interactions. However, with the complete of the formulation of the SM at the end of the 1970's, these two interactions became unified in what is known as the electroweak interactions. The unification is accomplished utilizing the symmetry group $SU(2)_L \times U(1)_Y$ where L denotes the left chirality and Y stands for hypercharge (18). The hypercharge is different from the electromagnetic charge. Under $SU(2)_L$ the left-handed chirality leptons and quarks are classified into three families as

$$\binom{v_e}{e}, \binom{v_\mu}{\mu}, \binom{v_\tau}{\tau}, \binom{u}{d}, \binom{c}{s}, \binom{t}{b} \tag{1.1}$$

While right-handed chirality charged leptons and quarks can be expressed as

$$e_R, \mu_R, \tau_R, u_R, d_R, c_R, s_R, t_R, b_R$$

The SU (2) $_L$ has three generators which can be expressed in terms of the three Pauli σ matrices as $T_a = \frac{1}{2}\sigma_a$. Under SU (2) $_L$ local gauge transformation we have (18).

$$\psi(\chi) \longrightarrow \psi'(x) e^{i\theta a(x)Ta} \psi(x), a = 1,2,3 \tag{1.2}$$

Under the above transformation, the Lagrangian is not invariant. One need to introduce three-gauge field in order to restore the invariance of the Lagrangian (18). These gauge fields must transform as follows

$$W_\mu^a(x) \longrightarrow W'^a_\mu(x) = W_\mu^a(x) + \frac{1}{g}\partial_\mu \theta^a(x) + \in^{abc} W_\mu^b(x)\theta^c(x), a = 1,2,3 \tag{1.3}$$

Here g is the coupling constant associated with SU (2) $_L$ gauge symmetry and $\boldsymbol{\epsilon}$ is structure constant. Next, we replace the usual derivative in the Lagrangian with the covariant one (18) i.e.

$$\partial_\mu \longrightarrow D_{\mu=} \partial_\mu - igT_a W_\mu^a(x) \tag{1.4}$$

The real gauge $W_\mu^a(x)$ fields have kinetic terms that must be added to the Lagrangian. These terms can be written as (19).

$$\mathcal{L} = -\frac{1}{4} W_{\mu v}^a W_a^{\mu v} \tag{1.5}$$

where $W_{\mu\vartheta}^\alpha$ a field strength tensor defined as

$$W_{\mu v}^a = \partial_\mu W_v^a - \partial_v W_\mu^a \tag{1.6}$$

So far, we have four new gauge fields associated with the two-gauge groups SU (2)$_L$ and U (1) $_Y$. They are three for SU (2)$_L$ namely, the fields (W_1, W_2, W_3) and one for U (1)$_Y$ the (B_μ) field. The covariant derivative of the unified SU (2) $_L$ x U (1) $_Y$ local gauge symmetry is given as (19)

$$D_\mu^{L,R} = \partial_\mu - igI_a^{L,R} W_\mu^a - i\frac{g'}{2} Y B_\mu, \quad I_a^L = \frac{1}{2}\sigma_a, \; I_a^R = 0 \tag{1.7}$$

The last term of the Eqn. 7 expresses the fact that we do not need right component because SU (2)$_L$ does not act on right handed fermions. The charged weak gauge bosons are combinations of the gauge fields W_μ^1 *and* W_μ^2 and given as

$$W^{\pm\mu} = \frac{W_1^\mu + W_2^\mu}{\sqrt{2}} \tag{1.8}$$

On the other hand, the photon and the Z boson are combinations of the gauge fields B_μ and W_μ^3:

$$A_\mu = B_\mu \cos\theta_\omega + W_\mu^3 \sin\theta_\omega\,, Z_\mu = -B_\mu \sin\theta_\omega + W_\mu^3 \cos\theta_\omega \tag{1.9}$$

where θ_ω is the Wienberg θ angle (19).

1.3 Triple Gauge Coupling (TGCs) In The SM

Among the very interesting features of the SM are the Triple Gauge Couplings. They arise due to the non-Abelian structure of the SU(2)$_L$ and SU(3)$_C$ gauge symmetries. They are responsible for the gauge boson self-interactions as can be remarked from the last term appearing in the equation (7).

$$g\epsilon_{ijk} W_\mu^j W_\upsilon^k$$

$$W_{\mu\upsilon}^i = \partial_\mu W_\upsilon^i - \partial_\upsilon W_\mu^i + g\epsilon_{ijk} W_\mu^i W_\upsilon^k \tag{1.10}$$

where ϵ_{ijk} is the SU (2) structure constant which vanishes when two indices are equal, Thus, this term admits only self-interactions between different types of bosons which explains why the SM allows at tree level only the self-interaction of the charged gauge bosons giving rise to the vertices W+W−Z(γ). On the other hand, neutral triple gauge boson vertices are forbidden in the SM and hence no $Z\gamma Z$ and $ZZ\gamma$ vertices present at tree level. In searching for these neutral triple couplings, any deviations from these SM expectations will be a sign of new physics beyond SM (20).

An example of a vertex representing a neutral triple gauge bosons interaction, is shown in Figure 1.3. As stated above, this vertex is forbidden in the SM at tree level. However, it can be obtained at loop level and thus is expected to be very small. In addition, it can be enhanced in some classes of new physics beyond SM and hence it is possible to search for such couplings when analyzing multi-boson final states. In the literature, there are several approaches to parameterize such couplings. There are two common approaches to investigate these neutral triple couplings. The first approach is the anomalous coupling approach (21, 22, 23, 24) and the second one is the Effective Field Theory (EFT) approach (25). In the next chapter we review the first approach used in the study carried out in this thesis.

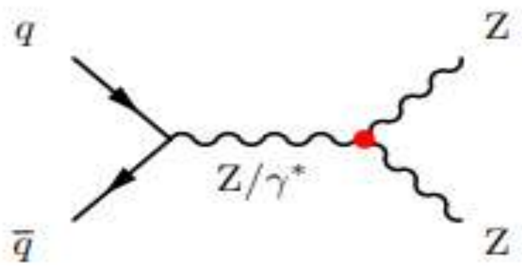

Figure 1.3. ZZ production via s-channel which is forbidden in Standard Model (26).

1.4 Missing Part In SM

The standard model has been widely accepted to be in an outstanding agreement with lot of confirmed experimentally observations up to date. These include, for instances, the observation of the gauge bosons W and Z, with masses and decay properties that precisely

match the SM predictions. Additionally, the discovery of the Higgs particles at LHC completed the spectrum of particles as expected within SM with three fermions generations (20). In fact, the SM is extraordinarily successful in explaining with high accuracy most aspects of the nature at the electroweak scale. However, even with these impressive experimental confirmations of the predictions of the SM, there are quite number of phenomenological and theoretical major issues that cannot be addressed in the SM. This implies that the SM cannot be the ultimate theory of Nature. Hence, the SM can be thought as only an effective low energy limit of a more fundamental theory. For any such theory beyond SM, it is obligatory to exactly reproduce the SM at the electroweak scale. In the following section we highlight the most relevant issues that cannot be addressed in the framework of the SM.

On the theoretical side, the SM gauge structure does not include a gauge group accounting for the gravity. As a consequence, SM cannot be valid at energy scales above Planck scale $M_{Pl} \sim 10^{19}$ GeV. Additionally, the SM does not have a mechanism for generating neutrino masses and no viable candidate in the SM that cannot play the role of the Dark Matter (DM). Among the other theoretical problems that SM faces what is known as the naturalness problems of the Higgs boson in the SM. The problem arise due to the significant scale differences exists between the Higgs and the Plank mass and referred as the Hierarchy problem. One of the other main problems is related to the cosmological baryon asymmetry of the universe. This asymmetry originates due to the presence of more matter than anti-matter in the universe. One of the main possible reasons behind this asymmetry is the strength of the charge conjugation-parity (CP) violation which in the SM is not enough to account for this asymmetry (21).

At theory level, there are many doubts about accepting the SM as being a fundamental theory. One of these doubts is related to the number of free parameters in the SM which is 19. The value of these parameters cannot be predicted by the SM and consequently, they have to be measured experimentally. In addition, with this large number of free parameters, any description of nature based on the SM will be so complicated.

Having accepting that the SM cannot be a fundamental theory of nature, it is common attempts to look for alternative theoretical models seeking for addressing the raised questions not answered by the SM. These alternative theories or models are known as beyond standard model physics or sometimes they are called extensions of the SM. In the next chapter we give a brief introduction to the main directions for constructing such theories or models (21).

2. ANOMALOUS COUPLINGS APPROACH FOR TRIPLE GAUGE COUPLINGS.

Alternative beyond standard model physics can be constructed upon enlarging some sectors or symmetries in the SM. For instances, enlarging the gauge symmetry of the SM by adding new gauge symmetry groups (27). Another possibilities can be achieved by enlarging the Higgs Sector through adding new singlet scalars, new doublets and so on (28,29). Another theories or models can be formulated by enlarging the matter content of the SM by adding new fermions, new gauge bosons etc.… (30). In other classes of beyond SM physics, the space-time dimensions can be enlarged by adding new dimensions such as in Extra-dimensions and string theory (31) while in others the Lorentz Symmetry can be enlarged as in Supersymmetry (32). Gravity also can be incorporated with the other three mean forces as was done in Supergravity (33). Direct searches for new physics beyond SM at current experimental facilities results nothing up to date. This will push for making new collides that have high center of mass energies and integrated luminosities to be constructed at future and boosting the search. A novel search can be done through investigating the neutral triple gauge couplings which are vanishing at tree-level in the SM as we will discuss in the following.

The great finding of the Higgs boson LHC confirmed the Electroweak Symmetry Breaking (EWSB) essential for generating masses for quarks, charged leptons, the $W^{\pm}$ and the Z boson (34). However, the EWSB mechanism is still not fully understood. To do this you need an accurate measurement of Higgs self-couplings, Higgs to gauge boson couplings and gauge boson self-couplings. In this thesis we shall restrict ourselves to Triple Gauge boson Couplings (TGC). The cubic and quartic self-couplings of the electroweak gauge bosons exist in the SM due to the presence of the non-abelian gauge symmetry, and thus are completely fixed by the electromagnetic coupling constant e and the weak mixing angle sin θ_W. This in turn leads to precise predictions for these couplings within SM. This, however, is not the case in a general BSM physics. As a consequence, processes that are sensitive to gauge boson self-interactions are important tools used to search for new physics beyond the SM. Moreover, the absence of neutral aTGC at the LHC and future colliders will give a huge support to the EWSB. On the other hand, the presence of the neutral aTGC will be an indication of a possible new physics required to explain several phenomena including for instances CP violation, Baryogenesis, dark matter.

Based on the discussion above, the ZZ and Zγ production are the two leading processes where one can study the neutral aTGC. Any deviations of the couplings from the expected values would imply the existence of new physics beyond the SM. In this thesis we concentration on a detailed investigation of the anomalous ZZV (V=Z, γ) couplings in ZZ production at future hadron-hadron colliders (34).

The SM in the framework, at the patron level, the process $pp \rightarrow ZZ$ at tree-level originate from the Feynman diagrams shown in Figure 2.4. The addition of the graph in Figure 2.2 is crucial to include the aTGC in the calculations of the process $pp \rightarrow ZZ$ at tree-level.

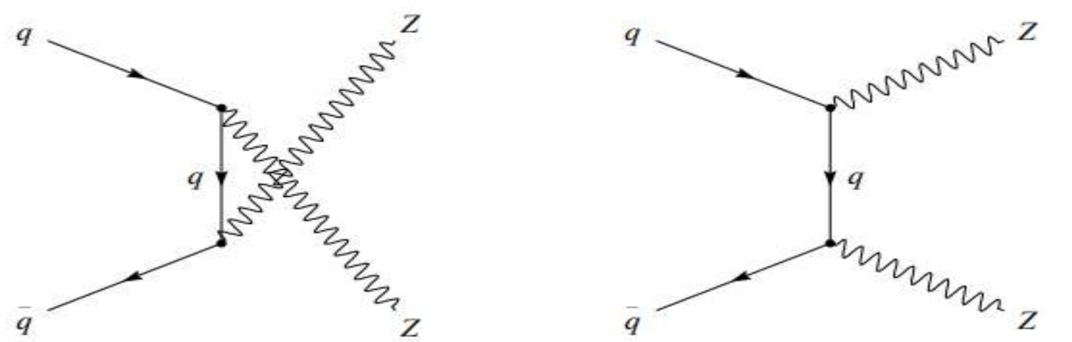

Figure 2.1. The Feynman diagrams for the tree level procedure contributing to $pp \rightarrow ZZ$ in the SM (22).

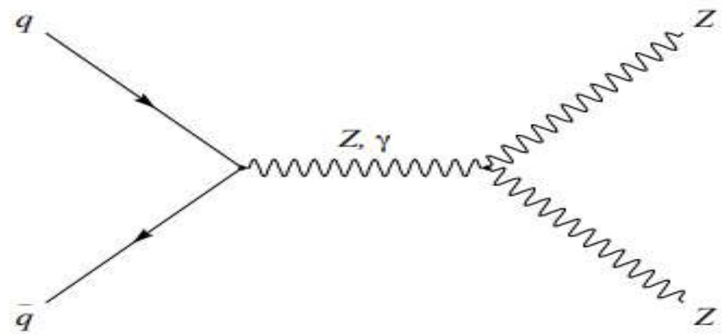

Figure 2.2. Contributions of ZZZ and $ZZ\gamma$ diagrams to $qq^{-} \rightarrow ZZ$ (22).

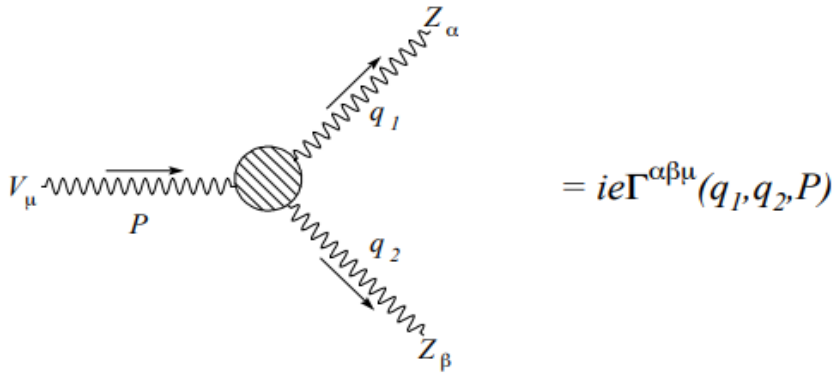

Figure 2.3. Feynman rule for the general ZZV $(V = Z,\gamma)$ vertex (22).

The neutral aTGC can be achieved through extending the SM to include higher dimension effective operators (35,36). It starts to appear with dimension-8 onward and thus one expects that their effect will be very small at low energies. An alternative way is to parametrize the neutral aTGC with dimension-6 (and 8) form factors in a model-independent way as discussed in Ref. (14). A Lagrangian that describes the aTGCs can be obtained upon taking into account all Lorentz and $\mathrm{U}(1)_{em}$ invariant terms. Generally, there is an infinite number of such terms bearing in mind that higher order derivatives can be considered. However, as commonly considered in the literature, taking only lowest number of derivatives (lowest-order) reduces the number of such terms. In the case that all three bosons are on-shell, it is direct to show that the Bose statistics and the Gauge Invariance condition for V= γ,Z results in vanishing vertices. As a consequence of all the aforementioned requirements, the effective Lagrangian for the on-shell ZZ final state can be expressed as (37):

$$\mathcal{L}_{VZZ} = -\frac{e}{M_Z^2}[f_4^V(\partial_\mu V^{\mu\beta})Z_\alpha(\partial^\alpha Z_\beta) + f_5^V(\partial^\alpha V_{\sigma\mu})\check{Z}^{\mu\beta}Z_\beta] \qquad (2.1)$$

There are two drawbacks regarding the anomalous couplings approach. Firstly, the Lagrangian includes only the lowest order terms. Secondly, the unitarily violation takes place when one computes the tree level amplitudes (37). However, these two drawbacks can be partially overcome by working in the momentum space in an analogy to the position space Lagrangian. This is known as the vertex function framework. The ZZV neutral $aTGC$ vertices can be expressed as (37)

$$g_{ZZV}\Gamma^{\alpha\beta\mu}_{ZZV} = e\frac{P^2-M_V^2}{M_Z^2}[if_4^V\left(P^\alpha g^{\mu\beta}+P^\beta g^{\mu\alpha}\right)+if_5^V\epsilon^{\mu\alpha\beta\rho}(q_1-q_2)_\rho \quad (2.2)$$

where $V = Z, \gamma$ will hereafter stand for the off-shell Z or γ bosons, M_Z is the Z-boson mass and e is the proton charge. The overall factor $(P^2 - M_V^2)$ appears in Eq. (12) is a consequence of Bose symmetry for ZZZ couplings. The couplings f_i^V (i = 4, 5) are dimensionless complex functions of q_2^1 , q_2^2 and P^2 (21). The couplings f_4^V is CP-violating coupling while f_5^V is CP-conserving. It should be remarked that no interference terms between the CP-violating couplings and the standard model will be included in the square of the matrix element necessary for the cross-section evaluation.

$$ie\Gamma^{\alpha\beta\mu}_{Z\gamma V}(q_1,q_2,q_3) = \frac{-e(q_3^2-m_V^2)}{M_Z^2}\{h_1^V\left(q_2^\mu g^{\alpha\beta}-q_2^\alpha g^{\mu\beta}\right)-\frac{h_2^V}{M_Z^2}q_3^\alpha[(q_3q_2)g^{\mu\beta} - q_2^\mu q_3^\beta - h_3^V\epsilon^{\mu\alpha\beta\rho}q_{2\rho}-\frac{h_4^V}{M_Z^2}q_3^\alpha\epsilon^{\mu\beta\rho\sigma}q_{3\rho}q_{2\sigma}\} \quad (2.3)$$

The h_1^V and h_2^V are CP-violating couplings while the h_3^V and h_4^V are CP-conserving couplings.

3. DETAILS OF FUTURE HADRON COLLIDERS

High energy hadron colliders has proven to be very useful tools for discoveries at the energy frontier from starting from the SppS collider to the Tevatron collider and nowadays the LHC. It is expected that, they will be unchallenged for the near future. In fact, a new era for particle physics has been reached as a result of the discovery of Higgs boson at the LHC (38). The discovery implies that the next key challenge for collider physics is to understand the origin of the electro-weak symmetry breaking mechanism. This can be achieved upon answering questions like up to which level of precision does Higgs boson behaves as exactly predicted by the SM? Additionally, the question regarding the existence of new particles required for solving the electroweak (EW) naturalness problem.

CERN has approved several options for upgrading the LHC. These future upgrades of the LHC include an upgrade with higher luminosities (HL-LHC) , an upgrade with higher energy (HE-LHC) and a new proton collider with collisions taking place at a center of mass energy up to 100 TeV (FCC-hh) (38).

The statistical gain in running the LHC collider at constant luminosity is expected to continuously decrease. As a result, the LHC will be in need for increasing of its luminosity to continue probing new phenomena and high mass scale (39). This new phase of the LHC is referred as the High Luminosity LHC (HL-LHC). In this phase, the machine will be prepared to achieve the astonishing threshold of 3000 fb^{-1} of integrated luminosity during the first decade of its operation. It is well known that the precision of several key measurements at LHC can be increased through utilizing the upgrades to high luminosity colliders. Consequently, this will give the possibility to uncover rare processes. Moreover, it will guide and validate the improvement in formulating theoretical models and hence decrease the systematic uncertainties in the interpretation of the data.

As declared by the CERN Council, the project is now considered the first priority of Europe (39). The superconducting (SC) magnet technology plays a crucial role regarding the LHC and proton proton colliders. The LHC, for instances, relied on approximately 40 years of development of SC technologies using $Nb\,Ti$ wire.

A favored way to increase the luminosity of the LHC to achive the desired HL-LHC collider is to reduce the β^* parameter of the beam optics, controlling the beam focusing at interaction point (IP), by means of larger aperture triplet magnets in the interaction area. Such design necessitates the presence of quadrupoles whose aperture is 150 mm and with peak field in excess of 12 T, beyond the limits of the $NbTi$ conductor (40).

Magnet technologies has a central role in any upgrade of the LHC toward higher energies. In addition to the oriented program of engineering development, the individual programs related to the long-range research focusing on magnetic materials and structures are of significant importance (40).

Advances in magnets with operating magnetic fields of 14–16 T or beyond are quite essential for the long-range future high energy pp colliders (41). For instances, the FCC-hh collider with collision energy 100 TeV and an 80 km tunnel, the target operating magnetic field is of 20 T dipoles. On the other hand, a 100 km tunnel will provide the same collision energy of 100 TeV with reduced field of just 14–16 T (42). One can notice that a large tunnel may also open up the possibility of an e^+ e^- storage ring as a Z, W and Higgs factory and of e p colliders (42).

Colliders with center of mass energy beyond that of the LHC will face significant challenges. Among these challenges, the emission of beam synchrotron radiation. This is expected to be at least 20 times greater in comparison to the corresponding one of the LHC (43). Regarding the HE-LHC a solution based on a beam screen at 40–60 K has been checked. The results show that the solution has no major drawbacks, although one should consider carefully developing the design, the engineering and prototyping to prove this solution. On the otherhand and for a 100 TeV machine such as FCC-hh collider, sealing with the synchrotron radiation will become a major challenge which necessitates further detailed study (43).

3.1 HL – LHC

One of the proposed upgrades of the LHC is the so-called High Luminosity Large Hadron Collider (HL-LHC). In the period starting from 2011 till the year 2020, the project was directed by Lucio Rossi and right after that by Oliver Brüning (44). The HL-LHC project is aiming to improve the performance of the LHC potential for discoveries after 2027. This will be accomplished through increasing the luminosity by a factor of 10 in terms of the LHC's designed value (44). Luminosity is one of the important factors regarding the performance of a collider. As it is known, the Luminosity is proportional to the number of collisions that occur in a given time interval. As a consequence, the higher the luminosity, the more collected data that can help in observing rare processes (45). The HL-LHC is planned to operate from the end of 2027. It will help physicists to study the known mechanisms, such as Higgs mechanism, in greater detail and it may lead to observations of rare new phenomena. For instances, the HL-LHC can produce at least 15 million Higgs bosons each year of operation. This has to be compared with the nearly three million Higgs bosons produced from the LHC in 2017 (45).

In 2013, the HL-LHC project was declared as the top priority of the European Strategy for Particle Physics. The first stage of the project started in 2011. The design study of the collider came to a close in October 2015 while the civil-engineering work was initiated in April 2018. The project is led by CERN with the participation of 29 institutions from different 13 countries around the world (46).

Project timeline

Below we list the time line of the HL-LHC proposal till 2020.

- 2011: The approval and starting of the FP7 HL-LHC design study.
- 2014: Publishing the first preliminary report on the design study.
- 2015: The technical design report, budget and schedule of the project was made available.
- 2016: The approval of the initial budget and schedule of the project by CERN Council.
- The parts of hardware including components and models were validated in the period 2018 – 2020.
- Civil engineering constructions and prototyping process were continued till the year two thousandth twenty one.

3.2 HE – LHC

The HE-LHC project is a pp collider, planned to work at center of mass energy $\sqrt{s} = 27$ TeV. It is designed to collect data of order 15 ab^{-1} during a period of 20 years of operation. It use the current LHC tunnel and will rely on the 16 T magnet technology which will be advanced for FCC-hh collider (47).

The center of mass energy planned 27 TeV, of the HE-LHC collider, lies below the 100 TeV target of the FCC-hh. However, the energy and luminosity of the HE-LHC constitutes an important improvement compared to the HL-LHC reach (48). In fact, the discussion of the capabilities for HE-LHC related to the exploration of physics should not be done through a comparison with the FCC-hh project. Rather, one should consider the expected costs and benefits that it will bring when the HL-LHC finishes its period of operation. The potential returns of the HE-LHC can be summarized in the following specific four areas (48):

1. Broadening the HL-LHC mass reach in direct searches for new nonstandard particles, by nearly doubling the reach in mass.
2. Foundation the mechanism of the symmetry-breaking in the Higgs sector of the SM.
3. Reaching a high accuracy of the HL-LHC measurements in the electroweak and flavor sectors. This will have a consequence leading to a better indirect sensitivity to look for new physics at high mass scales, and also to search directly for final states such as dark matter (DM).
4. Investigating the properties of the potential future LHC discoveries with large detail, confirming initial signs of discoveries from the LHC, or recognizing the exporter of new phenomena such as DM.

It should be noted that, only future data can allow to qualify and quantify the importance of the fourth space in the planning for the HE-LHC (48). At present, only a few scenarios can be taken as examples. In the workshop “The physics of HL-LHC, and perspectives at HE-LHC”, detailed discussions and evaluations of the physics program at the HE-LHC has been presented (49).

3.3 The Future Circular Collider (FCC)

The FCC is one of the candidates of post-LHC collider. The FCC is planned to have an energy significantly much larger compared to SPS, the Tevatron, and the LHC circular colliders. It has three proposed scenarios each corresponds to a different type of colliders (50). The first one is a hadron-hadron collider (proton–proton and heavy ion) and it is known as the FCC-hh collider. The second one is an electron–positron collider known as the FCC-ee collider. The last one is a proton–electron collider which is referred to as the FCC-eh (50).

The energy-frontier future hadron colliders will have the chance for observation of mediators of possible unknown forces in the range of mass scale up to 30 TeV. These proposed colliders can extend the search for candidates of dark matter beyond the TeV scale. Moreover, they can search for supersymmetric partners of the quarks and gluons at masses up to 15-20 TeV. At these energy-frontier future hadron colliders also, the exploration of possible internal structure of the quarks can be performed at distances of order 10^{-21} m (51). Studies concerning the Higgs and gauge boson interactions are among the main important studies at these specific colliders. Such studies are planned to be carried out at energies well above the TeV scale. Consequently, they can provide a method to analyze in great detail the electroweak symmetry breaking.

The design of the planned FCC-hh collider allows each colliding beam to achieve total energy reaching 560 MJ and a center-of-mass energy equals to 100 TeV (to be compared with 14 TeV at LHC). CERN hosted a study about Future Circular Collider aiming to explore different scenarios of particle colliders. The aim of the study is to look for the best options regarding the increase of the center of mass energy and the luminosity compared to the existing colliders. Another goal is to advance the technical designs of the future linear electron-positron colliders (ILC and CLIC) (51).

The physics program at the FCC collider aims to search for candidates of dark matter particles that constitute about a quarter of the total energy of our observed universe. Particularly this can be carried out in the mass range GeV – 10's of TeV for a verity of many proposed models with dark matter candidates being the weakly interacting massive particles (WIMPs) (51).

The FCC collider can improve significantly the measurement of the electroweak precision observables (EWPO) which are significant for better understanding of the SM and can further direct the development of the theoretical side. Additionally, data of such measurements can be obtained with the help of some astrophysical/cosmological observations. In fact, the improved precision that is expected to be obtained from the FCC collider may increase the discovery potential for physics beyond the SM (51). One of the possibilities of the FCC-hh collider is to allow for the heavy-ion collisions. This will serve as an important tool for exploring the structure of the matter at conditions characterized by very extreme density and temperature (51).

The FCC-eh collider aims to explore the interaction point for electron with proton (51). The FCC-eh collider is planned to reach to huge center of mass energy through colliding a 50 TeV proton beam and electron beam that has energy close to 60 GeV. With this energy, it is expected to open new windows to investigate deep inelastic scattering processes. On the other hand, the deep inelastic scattering measurements, which will be carried out at the FCC-eh, can help to resolve the Parton structure with very large precision. In turn, this will lead to a per mille accurate measurements of the strong coupling constant. These measurements will further improve the sensitivity of search for new phenomena. In particular, this can be the case at higher masses. Based on the discussion above, one can look to the FCC-eh collider as a Higgs factory with a high-precision and also as being a powerful tool giving the opportunity to the discovery of new particles. Moreover, the FCC-he collider will contribute to the studies related to the interactions involving quarks and gluons, and possible further internal structure of matter present in our universe (51).

The preparatory phase for the FCC-hh collider is planned to start operation in the first half of the running stage of the FCC-ee. Then, when the operation of the FCC-ee collider stops, there will be a machine removal, limited activities regarding the civil engineering and modification related to the infrastructures. The next step after that is the installation of the FCC-hh machine and detector and commissioning which is expected to take about 10 years in total (51). The planned duration of the operation of the FCC-hh is 25 years (52). This long period can permit different technologies to be utilized in the construction of the collider. For instances, these include high-temperature superconducting magnets, improved machine parameters and reduced risks, all to be compared with the immediate construction after HL-LHC (52).

4. AIM AND SCOPE THE STUDY

The main purpose of this thesis is to represent the effect of CP violating (CPV) [f_4^{γ} ,f_4^{Z}], and CP conserving (CPC) [f_5^{γ} ,f_5^{Z}] anomalous triple gauge couplings through $pp \rightarrow$ ZZ process with subsequent decay channels of Z boson in anomalous coupling approach framework for future hadron-hadron colliders.

These effects are examined at the three energy stages of the future hadron-hadron collider; namely HL-LHC; HE-LHC; FCC-hh. which is plan to build at Conseil European pour Ia Recherché Nucleaire (CERN) in Geneva, Switzerland**.**

5. MATERIAL AND METHODS

Monte Carlo (53) simulation method play important role of high energy particle physics. The discovery and identification of BSM physics needs better simulation tools. General purpose matrix-element based event generators have been found in the literature. One of them is Calculator for High Energy Physics (CalcHEP) (54) package program. Other packages created to solve a similar problem are GRACE (55, 56, 57), HELAS (58), CompHEP (59), FeynArts/FormCalc (60, 61, 62), MADGRAPH (63, 64), HELAC-PHEGAS (65, 66, 67), WIHIZARD (68), and SHERPA (69,70).

In the current study, we inspect the sensitivity of the anomalous triple gauge couplings, $f_4^{\gamma}, f_4^{Z}, f_5^{\gamma}, f_5^{Z}$ via $pp \to ZZ$ process using the CalcHEP program after implementation of the vertex function. We use CalcHEP in all event generation in this thesis. We will give details of CalcHEP event generation in the next subsection.

5.1 Details Of CalcHEP Package Program

CalcHEP (71) is a software package for the automatic calculation of the Feynman diagrams related to a gıven process, integration over multi-particle phase space in addition to event simulation at parton level. In turn, this makes CalcHEP a useful tool to perform effective evaluation and simulation, at the parton level, of high energy physics collider processes.

The basic idea of CalcHEP is to offer an interactive environment enabling the user to proceed from the Lagrangian to the final distributions in an effective way and a high level of automation at the same time. The implementation of a new model, describing particle interactions, into CalcHEP can be achieved through writing a set of pure text model files (71). These files should contain details of the model such as the properties of the model particles, parameters of the model, and vertices expressing particle interactions. The CalcHEP package is composed of three parts allowing to conduct symbolic, numerical and batch evaluations. The first two parts of the package are expressed in the C programming language (72) where the symbolic part generates C codes for the calculated squared matrix elements which can be then used in the numerical estimations. The third part of the package is written in Perl.

5.1.1 Installation

The download of the package CalcHEP can be achieved following the link http://theory.sinp.msu.ru/~pukhov/calchep.html.

The installation of the CalcHEP package will be start once the user unpack the downloaded file (73). This can be done by

tar -xvzf   calchep_3.4.tgz

That generates the directory calchep_3.4 referred, here, as $CALCHEP. The next step is to compile CalcHEP. This can be done by typing cd into the $CALCHEP directory and do the run (73).

We will refer to this directory as $WORK. To install this directory, the user should run

. /mkWORKdir   <directory name>

where mkWORKdir is present at the $CALCHEP directory. This command establishes the directory $WORK= in addition to the subdirectories

models/ tmp/ results/ bin/

calchep is the shell script that can be utilized to start the symbolic session. It is invoked as ./calchep. On the other hand, CalcHEP batch is the shell script that can initiate a batch session. It is invoked as ./calchep-batch < batch. File **>** where batch refer to the file containing the batch instructions (74).

5.1.2 A Closer Look Into Model Files: Particles, Vertices, Parameters, Constraints, Libraries

(1) "Particles": This file contains the definitions of particles. For the SM, it is named as"prtcls1.mdl" and it is shown below (74).

```
prtcls7.mdl 〉 No Selection
ZZZ
 Particles
 Full  name    | A   | A+ | PDG     |2*spin| mass | width |color|aux| LaTex(A) | LaTeX(A+)   |
gluon         |G    |G    |21       |2      |0      |0      |8     |G   |g          |g
photon        |A    |A    |22       |2      |0      |0      |1     |G   |\gamma     |\gamma
Z-boson       |Z    |Z    |23       |2      |MZ     |wZ     |1     |G   |Z          |Z
W-boson       |W+   |W-   |24       |2      |MW     |wW     |1     |G   |W^+        |W^-
Higgs         |h    |h    |25       |0      |Mh     |!wh    |1     |    |h          |h
electron      |e    |E    |11       |1      |0      |0      |1     |    |e          |\bar{e}
e-neutrino    |ne   |Ne   |12       |1      |0      |0      |1     |L   |\nu_e      |\bar{\nu}_e
muon          |m    |M    |13       |1      |Mm     |0      |1     |    |\mu        |\bar{\mu}
m-neutrino    |nm   |Nm   |14       |1      |0      |0      |1     |L   |\nu_\mu    |\bar{\nu}_\mu
tau-lepton    |l    |L    |15       |1      |Ml     |0      |1     |    |\tau       |\bar{\tau}
t-neutrino    |nl   |Nl   |16       |1      |0      |0      |1     |L   |\nu_\tau   |\bar{\nu}_\ta
d-quark       |d    |D    |1        |1      |0      |0      |3     |    |d          |\bar{d}
u-quark       |u    |U    |2        |1      |0      |0      |3     |    |u          |\bar{u}
s-quark       |s    |S    |3        |1      |0      |0      |3     |    |s          |\bar{s}
c-quark       |c    |C    |4        |1      |Mc     |0      |3     |    |c          |\bar{c}
b-quark       |b    |B    |5        |1      |Mb     |0      |3     |    |b          |\bar{b}
t-quark       |t    |T    |6        |1      |Mt     |wt     |3     |    |t          |\bar{t}
==========================================================================================
```

Picture 5.1. prtcls1.mdl files of our models.

(2) **"Parameters":** This file contains all needed independent parameters of the considered model. For a given parameter a numerical value will be assigned to it. Below we show "vars1.mdl" corresponds to our model (74).

vars7.mdl 〉 No Selection

```
ZZZ
 Parameters
  Name | Value       |  Comment                                                               |
 EE    |0.3123       |Electroweak coupling. EE=0.31223 corresponds to alpha=EE^2/(4*PI)=1/128.9
 GG    |1.238        |Strong coupling. Value will be changed automaticaly in numerical session.
 alfSMZ|0.1184       |MS-BAR Srtong coupling at  MZ
 SW    |0.481        |MS-BAR sine of the electroweak mixing angle
 Mm    |0.1057       |muon mass
 Ml    |1.777        |tau-lepton mass
 Q     |100          | QCD scale
 McMc  |1.2          | Mc(Mc)  MS-BAR
 MbMb  |4.23         | Mb(Mb)  MS-BAR
 Mtp   |173          |t-quark pole mass
 MZ    |91.1884      |Z-boson mass
 Mh    |125          |higgs mass
 wt    |1.59         |t-quark width        (tree level 1->2x)
 wZ    |2.49444      |Z-boson width        (tree level 1->2x)
 wW    |2.08895      |W-boson width        (tree level 1->2x)
f4Z      |0           |
f5Z      |0           |
f4A      |0          |
f5A      |0           |
==================================================================================================
```

Picture 5.2. vars1.mdl file of our models.

(3) **"Constraints":** This defines the variables which depend on the parameters or the constraints that are defined previously. Their values are evaluated automatically once CalcHEP is running "func1.mdl". In the model considered in this work, our used constraints as listed below (75).

func7.mdl 〉 No Selection

```
ZZZ
 Constraints
 Name  |  Expression                                       |
CW     |sqrt(1-SW^ 2)     % cos of the Weinberg angle
MW     |MZ*CW             % W-boson  mass
GF     |EE^2/(2*SW*MW)^2/Sqrt2       % Fermi constant
LamQCD |initQCD(alfSMZ,McMc,MbMb,Mtp)
 Mb    |MbEff(Q)
 Mt    |MtEff(Q)
 Mc    |McEff(Q)
f4ZL   |f4Z
f5ZL   |f5Z
f4AL   |f4A
f5AL   |f5A
=========================================================
```

Picture 5.3. func1.mdl. file of our models.

(4) **"Vertices":** It includes actual particle interactions ("lgrng1.mdl"). The latest version of CalcHEP admits interactions with 4 particles. An interaction is

determined by a perfector and Lorentz. Our lgrng.mdl file, which is implemented with ZZV vertexes, is as follows (74).

```
lgrng7.mdl 〉 No Selection

ZZZ
 Vertices
A1   |A2   |A3   |A4   |         Factor            |  Lorentz part
    <|
G    |G    |G    |     |GG                         |m1.m2*(p1-p2).m3+m2.m3*(p2-p3).m1+m3.m1*(p3-p1).m2
G    |G    |G.t  |     |GG/Sqrt2                   |m1.M3*m2.m3-m1.m3*m2.M3
W+   |W-   |A    |     |-EE                        |m1.m2*(p1-p2).m3+m2.m3*(p2-p3).m1+m3.m1*(p3-p1).m2
W+   |W-   |Z    |     |-EE*CW/SW                  |m1.m2*(p1-p2).m3+m2.m3*(p2-p3).m1+m3.m1*(p3-p1).m2
W+   |W-   |Z    |Z    |-(EE*CW/SW)^ 2             |2*m1.m2*m3.m4-m1.m3*m2.m4-m1.m4*m2.m3
W+   |W+   |W-   |W-   |(EE/SW)^ 2                 |2*m1.m2*m3.m4-m1.m3*m2.m4-m1.m4*m2.m3
W+   |W-   |A    |Z    |-EE^ 2*CW/SW               |2*m1.m2*m3.m4-m1.m3*m2.m4-m1.m4*m2.m3
W+   |W-   |A    |A    |-EE^ 2                     |2*m1.m2*m3.m4-m1.m3*m2.m4-m1.m4*m2.m3
h    |W+   |W-   |     |EE*MW/SW                   |m2.m3
Z    |Z    |Z    |     |i/MZ^2                     |(p1.p1-p2.p2)*(f4ZL*(p3.m1*m2.m3+p3.m2*m3.m1)+f5ZL*eps(m3,m1,m2,p1-p2))
Z    |Z    |A    |     |i/MZ^2                     |(p1.p1-p2.p2)*(f4AL*(p3.m1*m2.m3+p3.m2*m3.m1)+f5AL*eps(m3,m1,m2,p1-p2))
```

Picture 5.4. lgrng.mdl. file of our models.

(5) "Libraries" includes codes to be defined by the user. In our model, we used default libraries in Calchep (74).

5.2 Cross Section For Process $pp \to ZZ$

The process $pp \to ZZ$ at tree level Feynman diagrams for the SM backgrounds and signal process are shown in Figure 2.1 and Figure 2.2, respectively. Figure 2.2 represent contribution of the anomalous triple gauge couplings. The total cross section of $pp \to ZZ$ process is evaluated using the CalcHEP package program after implementation of the following operators:

$$ie\Gamma_{ZZV}^{\alpha,\beta,\mu}(q_1,q_2,q_3) = \frac{-e(q_3^2 - m_V^2)}{M_Z^2}\left[f_4^V\left(q_3^{\alpha}g^{\mu\beta} + q_3^{\beta}g^{\mu\alpha}\right) - f_5^V \in^{\mu\alpha\beta\rho}(q_1 - q_2)_{\rho}\right] \quad (5.1)$$

During the cross-section calculations, we use the CTEQ6L Parton distribution function (75). To determine the region where aTGCs are separated from the SM at high center of mass energies in the $pp \to ZZ$ process, we give total cross section as a function of center of mass energies for four different aTGC couplings ($f_4^{\gamma}, f_4^{Z}, f_5^{\gamma}, f_5^{Z}$) in Figure 5.1. In this figure, only one anomalous coupling is kept to be different from zero. It is seen from this figure; the effects of the anomalous triple gauge coupling appear at the high energy values at the center of mass. Therefore, we focus on the future high energy hadron -hadron colliders, namely HL-LHC ($\sqrt{s} = 14\ TeV$), HE-LHC ($\sqrt{s} = 27\ TeV$), and FCC-hh ($\sqrt{s} = 100\ TeV$). To see the effect of each aTGC on the cross section, we obtained cross section versus coupling graphs for each future collider option. We plot total cross section as a function of anomalous triple gauge couplings [$f_4^\gamma, f_4^Z, f_5^\gamma, f_5^Z$], in Figure 5.2 for HL-LHC ($\sqrt{s} = 14\,TeV$), respectively. While obtaining these graphs, data were obtained by calculating the cross section values for each coupling value (after the others were set to zero), and also the quadratic fit functions applied to the obtained data were obtained. In these figures, the solid line shows the fit functions and circle points shows data calculated from CalcHEP. Similarly, the cross section versus couplings plots for other future hadron collider options are obtained in Figure 5.3 for HE-LHC, while Figure 5.4 for FCC-hh. Clearly from the figures, the cross sections corresponding to the couplings f_4^γ, f_4^Z are larger in comparison with f_5^γ, f_5^Z. This is attributed to the fact that the dependency of the squared matrix element on the terms f_5^γ, f_5^Z and f_4^γ, f_4^Z are not the same, due to the existence of the different overall factors in the vertex functions.

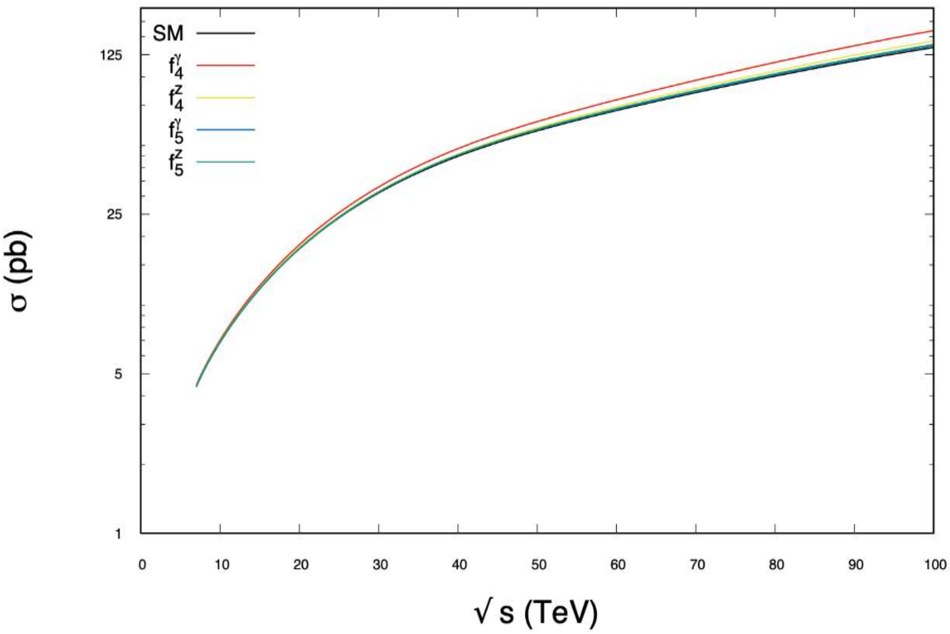

Figure 5.1. The cross section of the $pp \rightarrow ZZ$ as a function of center of mass energy for SM and anomalous TGC [$f_4^\gamma, f_4^Z, f_5^\gamma, f_5^Z$].

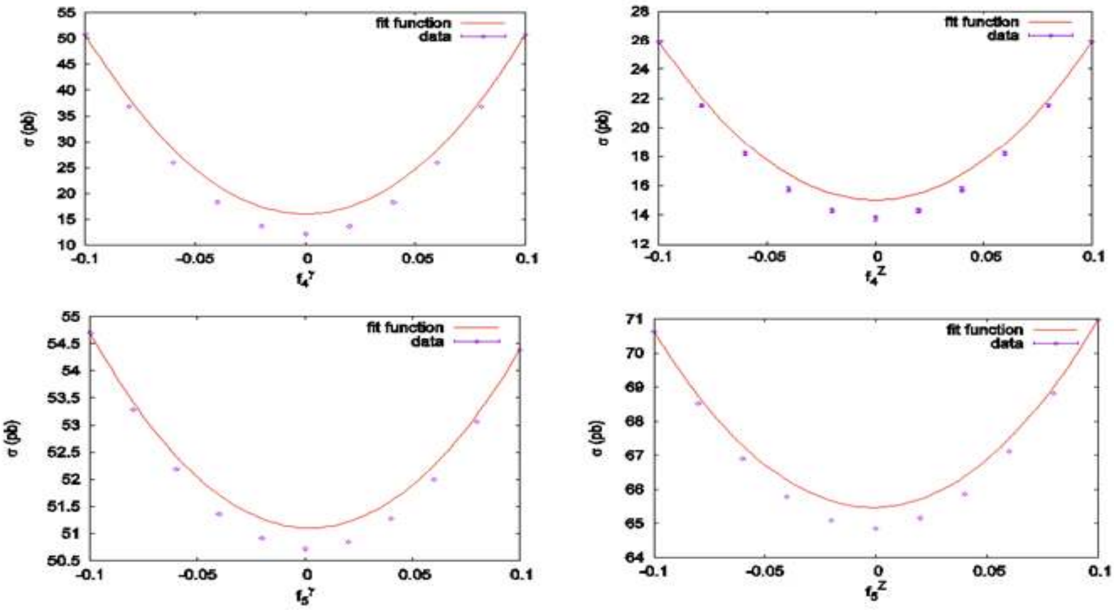

Figure 5.2. The variations of cross section (pb) as a function of $aTGC$ (f_4^{γ} , f_4^{Z}, f_5^{γ}, f_5^{Z}) at HL-LHC ($\sqrt{s}$ =14 TeV).

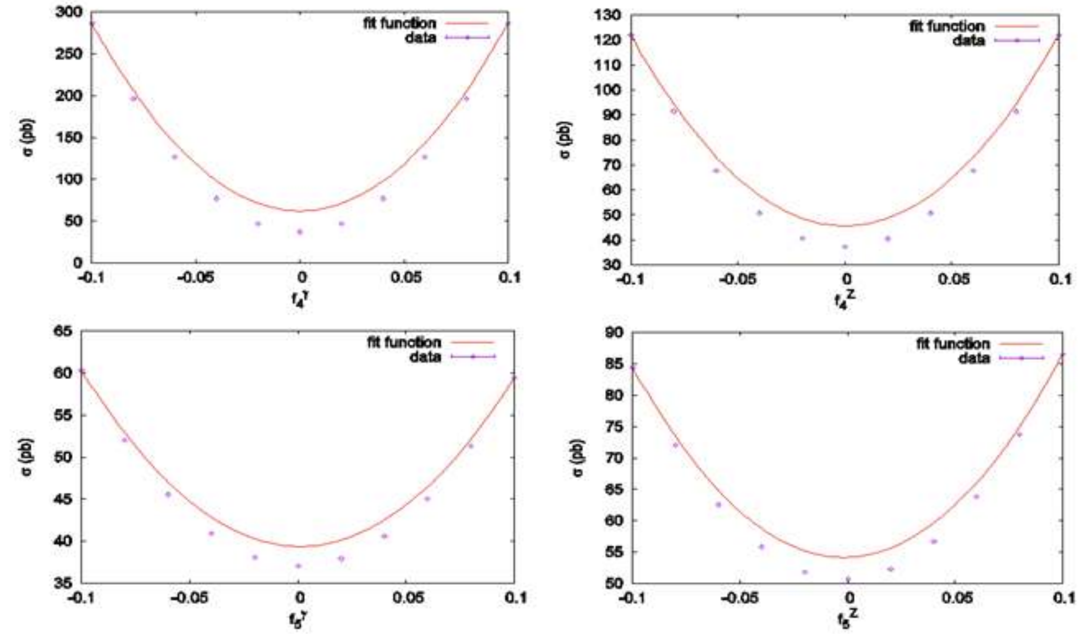

Figure 5.3. The variations of cross section (pb) as a function of $aTGC$ (f_4^{γ} , f_4^{Z}, f_5^{γ}, f_5^{Z}) at HE-LHC ($\sqrt{s}$ =27 TeV).

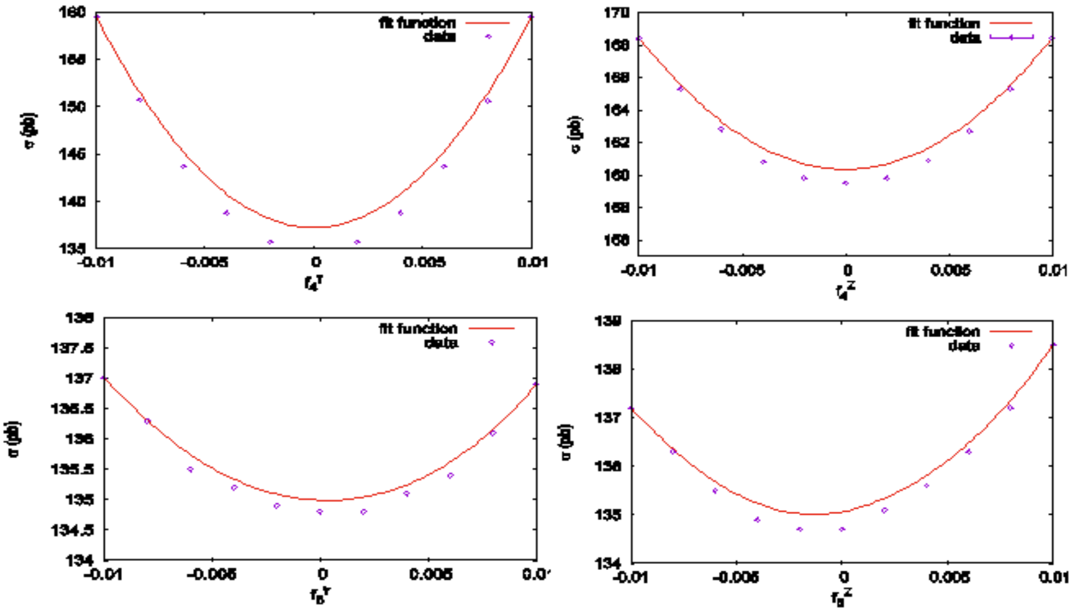

Figure 5.4. The variations of cross section (pb) as a function of $aTGC$ (f_4^{γ} , f_4^{Z}, f_5^{γ}, f_5^{Z}) at FCC-hh ($\sqrt{s}$ =100 TeV).

5.3 Kinematic Distributions Of The Final State Particles For $pp \rightarrow ZZ$ Process

The events for $pp \rightarrow ZZ$ process are generated by CalcHEP program using CTEQ6L Parton distribution functions of initial sate quarks and gluons. Parton showering and hadronization of the generated events with PYTHIA (76). After than the detector response are simulated by DELPHES (77) using HL-LHC, HE-LHC and FCC-hh detector cards. All events are analyzed by using the ExRootAnalysis (78) package with ROOT. In order to show the distributions of kinematic variables of final state particles, we generate events for standard model background (with final states being similar to the signal) and signal (with $f_5^{\gamma} = 0.01$) for demonstrative purpose at FCC-hh energy (√s=100 TeV).

Distributions are discussed the following subsections where one of the Z bosons decays to $\nu\nu$ while the other decays to e^+e^- or $\mu^+\mu^-$or qq.

5.3.1 $ll\,\nu\nu$ Final State

In this section, we demonstrate the behavior of kinematic variables of the final state charged leptons and neutrinos such as transverse momentum pT, rapidity, missing energy transverse (MET) and invariant mass of reconstructed Z boson from leading and sub leading electrons where they are oppositely charged. In figure 5.5 we show the transverse momentum (P_T) and pseudo-rapidity (η) at distributions of the final state leading (first row) and sub leading electron (at second row) for FCC-hh energy ($\sqrt{s}$=100 Tev), respectively similar figure for the final state leading and sub leading muon are shown in Figure 5.6 for the FCC-hh

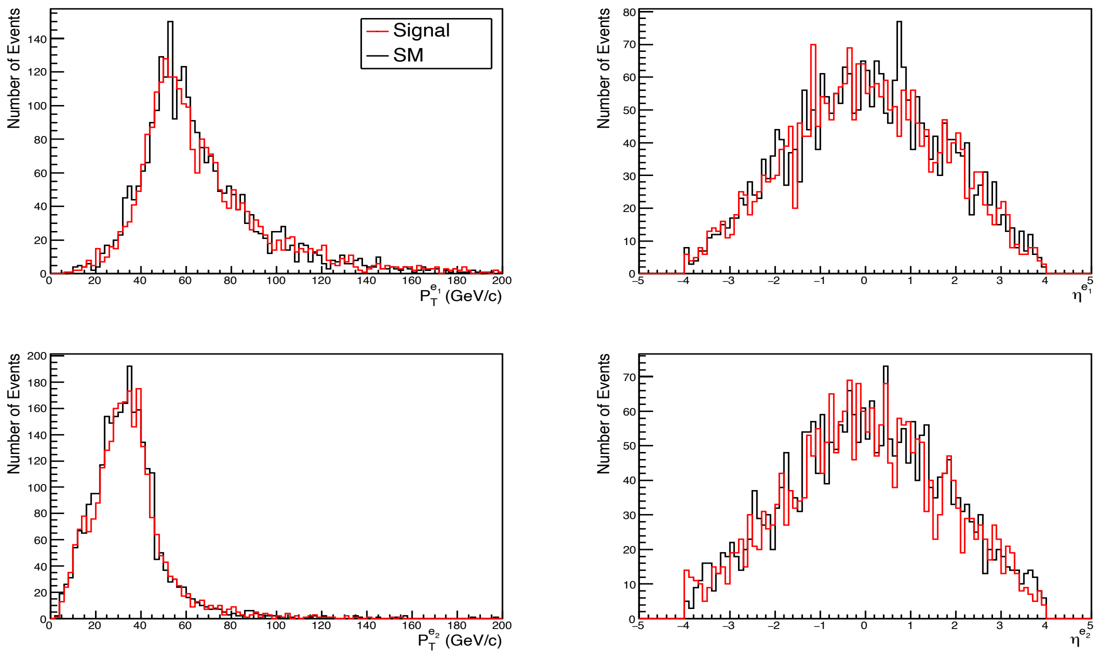

Figure 5.5. Distributions of the Transverse momentum pseudo-rapidity of the leading and sub-leading electron at FCC-hh.

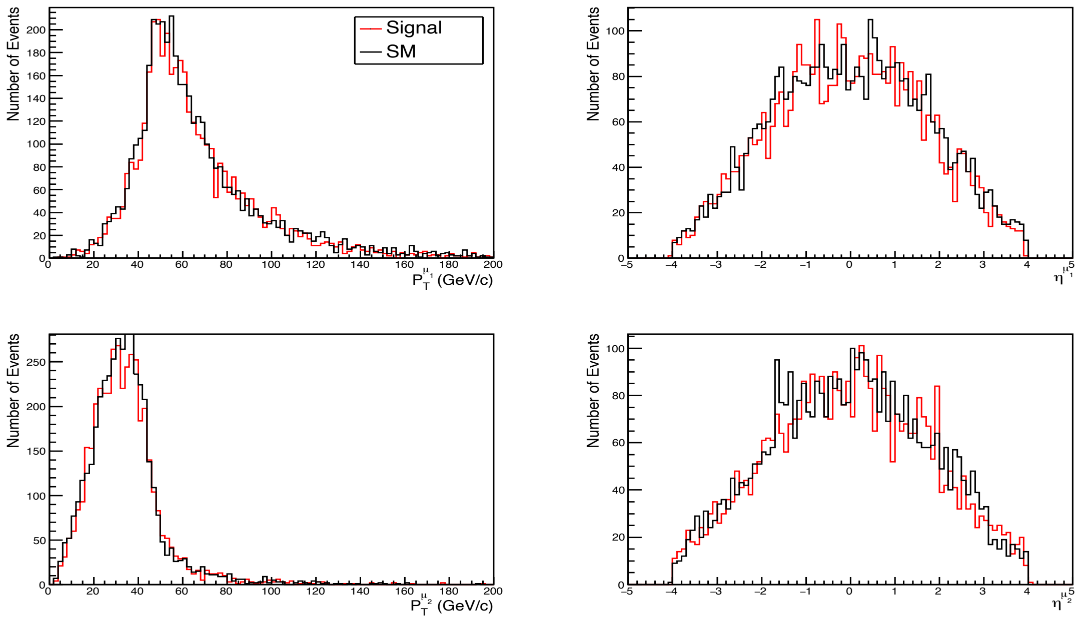

Figure 5.6. Distributions of the transverse momentum and pseudo-rapidity for the leading and sub-leading muon at FCC-hh.

In Figure 5.7 (Figure 5.8) we give the distribution of the invariant mass of reconstructed Z boson from electrons (muons) and missing energy transverse (MET) of the $l^+l^-\ \nu\nu$ channel for $pp \rightarrow ZZ$ process.

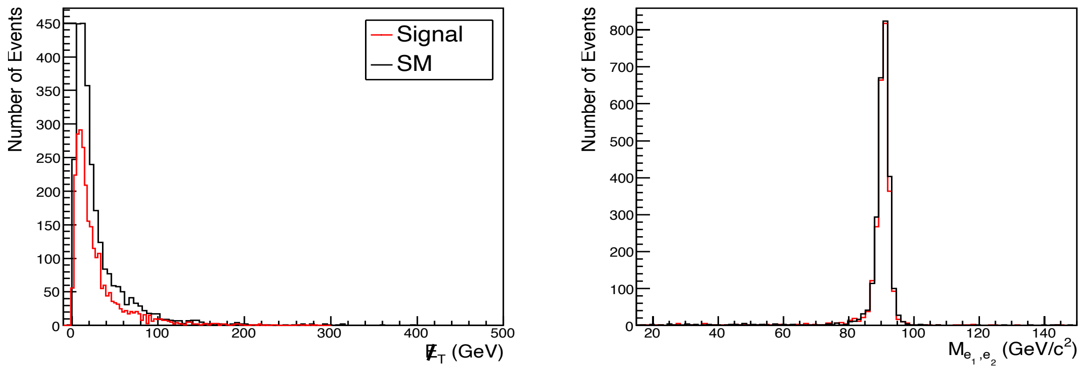

Figure 5.7. Distributions of the MET and invariant mass of the reconstructed Z boson from opposite charge of two electron at FCC-hh

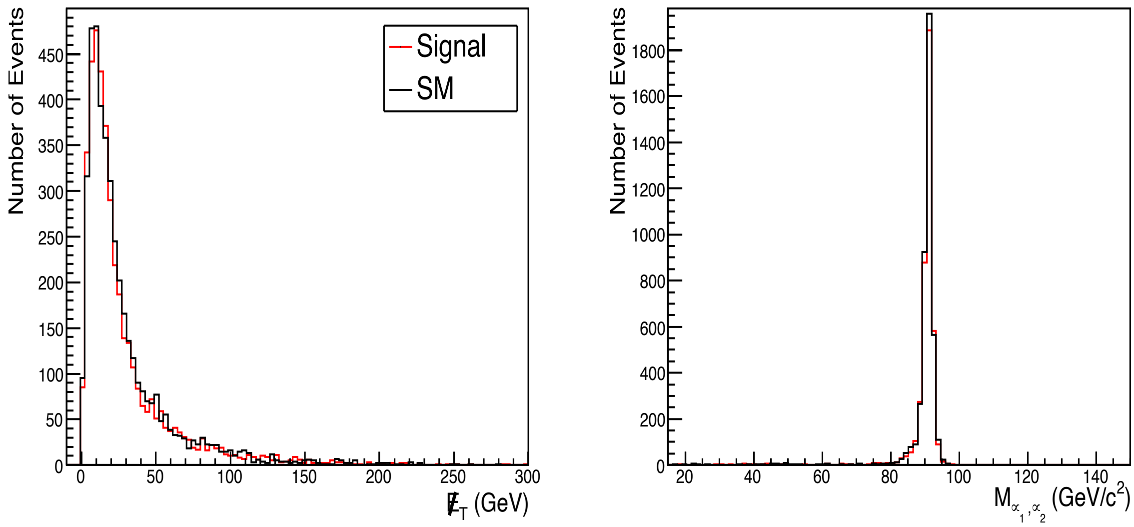

Figure 5.8. Distributions of the MET and invariant mass of the reconstructed Z boson from opposite charge of two muon at FCC-hh.

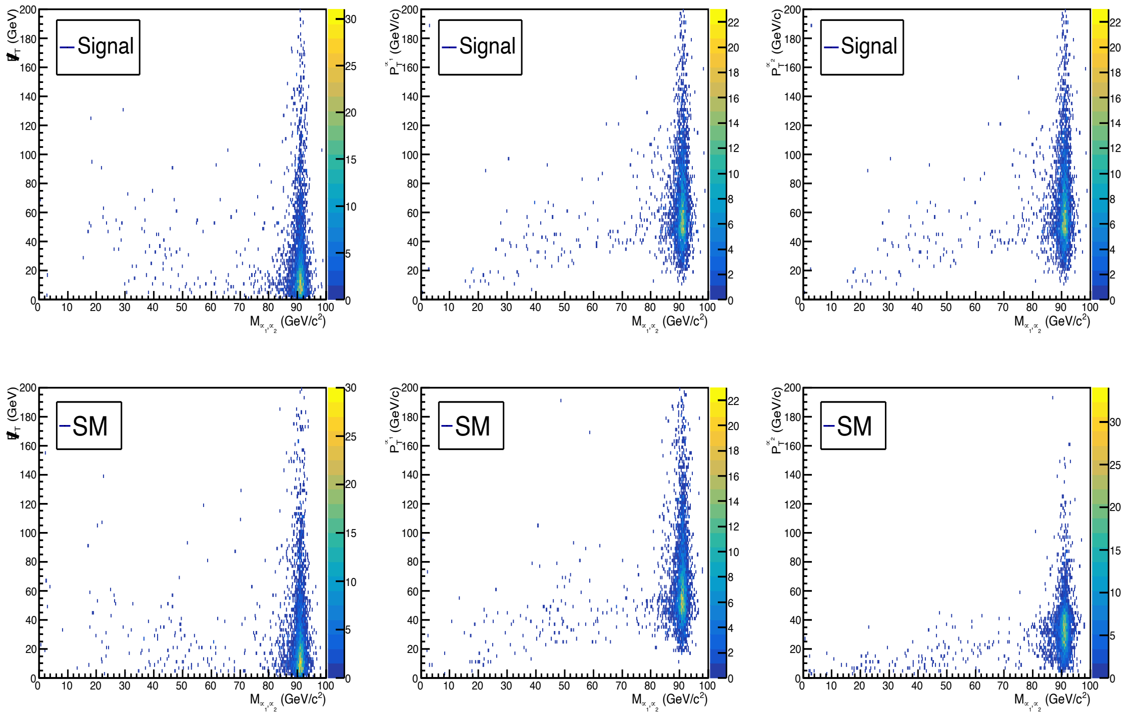

Figure 5.9. Distributions of the MET (first column), leading (second column) and sub-leading (third column) transverse momentum of electron versus mass of the reconstructed Z boson for signal (upper row) and background (lower row) at FCC-hh.

The phase space plots showing MET, leading and sub-leading electron versus the invariant mass distribution of the reconstructed Z boson from oppositely charged electron pairs are given in Figure 5.9 Plots similar to those Figure 5.9 obtained for the muon decay channels of Z boson as shown in Figure 5.10.

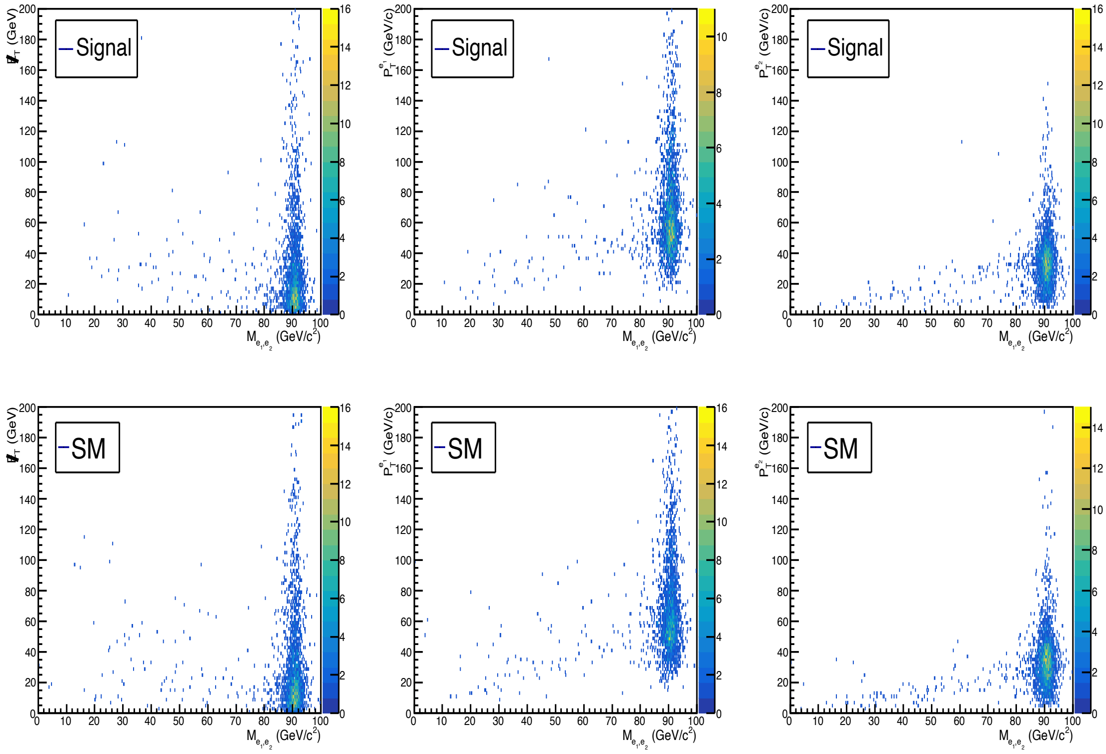

Figure 5.10. MET (first, Colum) leading and (second, Colum) sub-leading (three, Colum) transverse momentum of muon versus mass of the reconstructed Z boson for signal (upper row) and background (lower row) at FCC-hh.

In order to distinguish signal from background, the transverse momentum p_T^Z , $\cos\theta^Z$ (θ^Z polar angle), the opening angle in transverse plane (ϕ^Z) distribution of Z boson and ΔR distribution of e^+, e^- (μ^+, μ^-) pair originating from the decay of Z boson are given in Figure 5.11 (Figure 5.12) for electron (muon). Where the separation in pseudo rapidity azimuthal angle plane are defined as follows

$$\Delta R(l^+l^-) = [(\Delta\emptyset(l^+l^-) + (\Delta\eta(l^+l^-)^2]^{\frac{1}{2}} \quad (5.2)$$

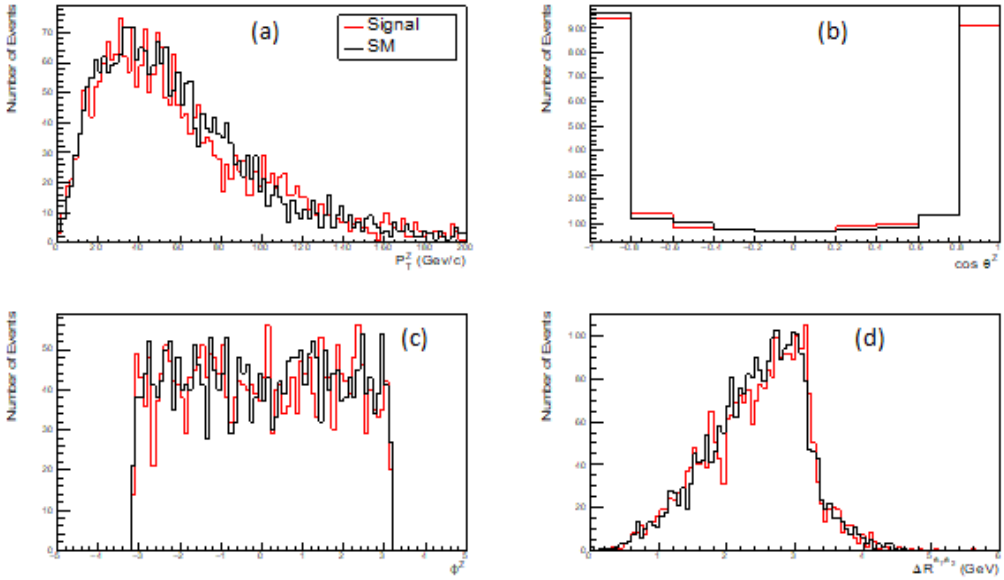

Figure 5.11. (a) Distribution of transverse momentum, (b) $\cos\theta^{Z}$, (c) ϕ^{Z} of reconstructed Z boson from two electron, (d) $\Delta R(e+, e-)$ for signal and background at FCC-hh.

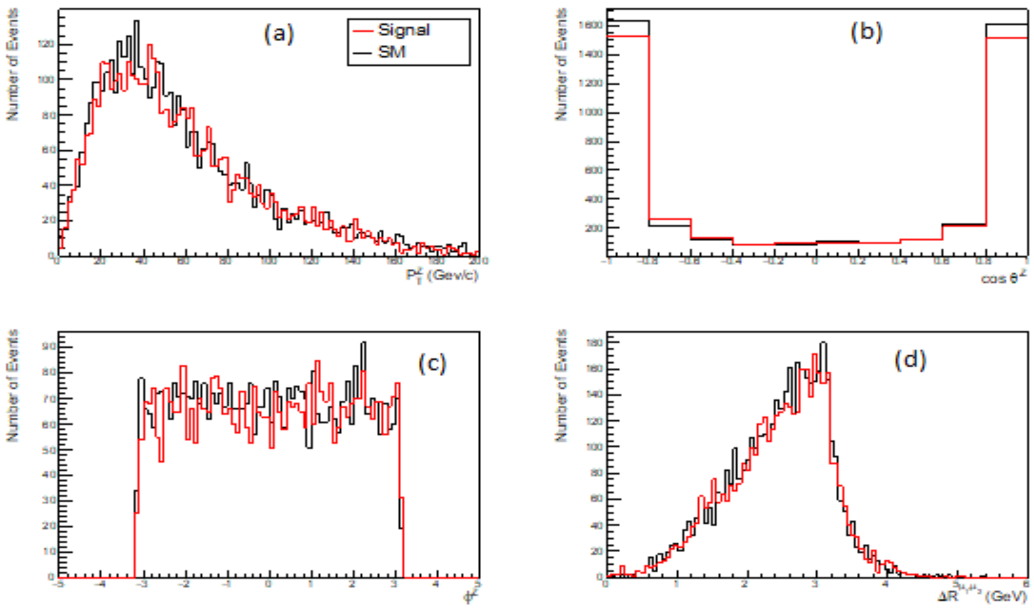

Figure 5.12. (a) Distribution of transverse momentum, (b) $cos\theta^{Z}$ (c) ϕ^{Z} of reconstructed Z boson from two muons and (d) ΔR (μ+, μ-) for signal and background at FCC-hh.

5.3.2 $qq\ \nu\nu$ Final State

Assumming decay of one of the Z boson hadronically, the other decays to neutrinos, we shall give the kinematical distributions of the jets generated in the final states of the process $pp \rightarrow ZZ$. Figure 5.13 displays the transverse momentum (P_T) and pseudo-rapidity (η) distributions of the final state leading (first row) and sub leading jets (at second row) for FCC-hh energy ($\sqrt{s}$=100 TeV), respectively. The invariant mass of reconstructed Z boson from jets and missing energy transverse (MET) of the semi-hadronic final state in ZZ production are given in Figure 5.14.

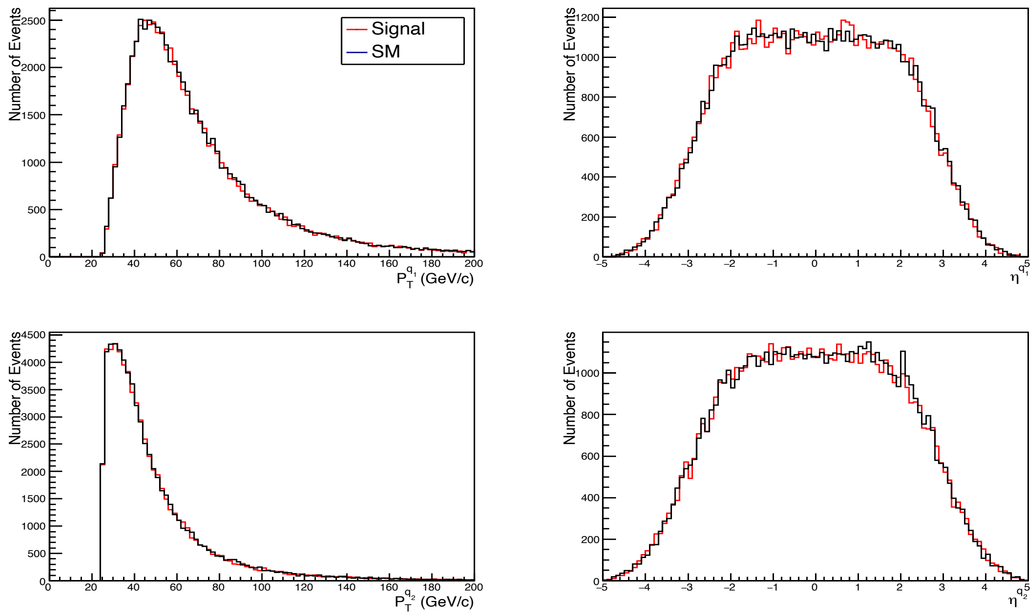

Figure 5.13. Distributions of the transverse momentum and pseudo-rapidity of the leading and sub-leading jets at FCC-hh.

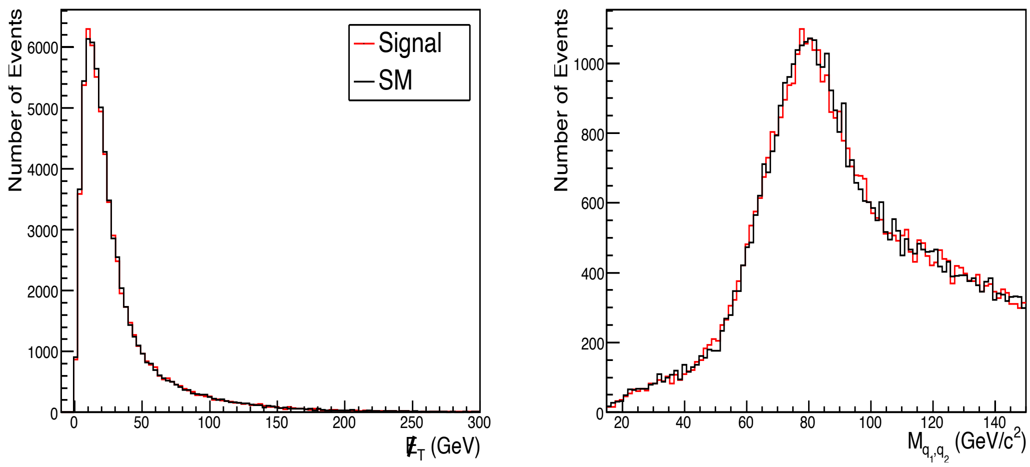

Figure 5.14. Distributions of the MET and invariant mass of the reconstructed Z boson from two jets at FCC-hh.

The phase space plots showing MET, leading and sub-leading jets versus the invariant mass distribution of the reconstructed Z boson from oppositely charged jets pairs are given in Figure 5.15

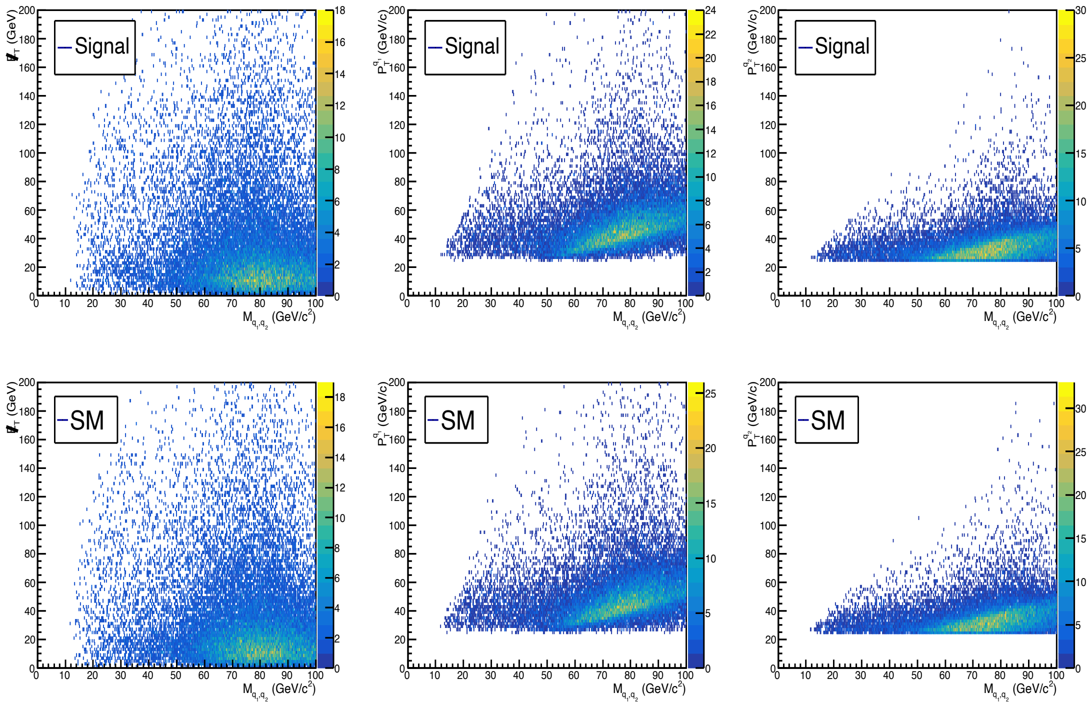

Figure 5.15. Distributions of the MET (first column), leading (second column) and sub-leading (third column) transverse momentum of jet versus mass of the reconstructed Z boson for signal (upper row) and Background (lower row) at FCC-hh.

The transverse momentum (a) p_T^Z , (b) $\cos\theta^Z$ $(\theta^Z\ is\ polar\ angle)$ scatting angle, (c) azimuth angle (ϕ^Z) distribution of Z boson and (d) ΔR distribution of q_1, q_2 pair originating from the decay of Z boson are given in Figure 5.16.

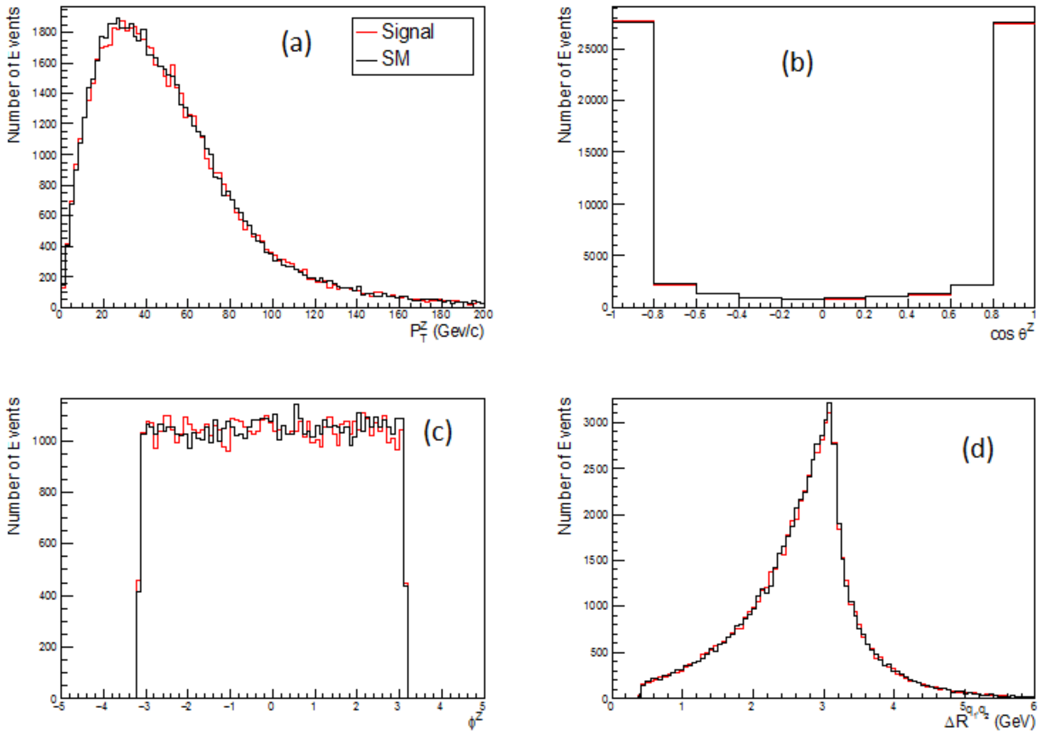

Figure 5.16. (a) Distribution of transvers momentum, (b) cosθ^Z where (θ^Z) is Polar angle, (c) azimuth angle (ϕ^Z) of reconstructed Z boson from two jets and (d) ΔR (q_1,q_2) for signal and Background at FCC-hh.

5.4 Sensitivity Limits For Anomalous Couplings

We present, in the following, the procedure applied to derive the sensitivity limits on the anomalous couplings. We evaluate the limits on $f_4^{\gamma,Z}$ and $f_5^{\gamma,Z}$ considering four signatures of ZZ production: decays to two leptons and missing energy; two leptons and two jets; two jets plus missing energy; and four leptons; at the set of the colliders presented before.

One of the well know method to show the sensitivities of the coupling in the literature is χ^2 criterion. The chi-square χ^2 is one of the most useful statistics for testing hypotheses when the variables are nominal (79)**.** Is a valuable analysis tool that provides considerable information about the nature of research data. The χ^2 function is defined as follows;

$$\chi^2 = (\frac{\sigma^{signal-}\,\sigma^{sm}}{\sigma^{sm}.\ \delta})^2 \qquad (5.3)$$

where σ^{signal} is the cross section in the presence of anomalous couplings and σ^{sm} corresponding SM background, $\delta = \frac{1}{\sqrt{N}}$ and N is number of events. We use following forms at number of events four signatures of ZZ production:

$$N = \sigma_{SM}. L_{int} . BR(Z \to l^+l^-). BR(Z \to vv) \text{ for } l^+l^-vv \,,$$

$$N = \sigma_{SM}. L_{int}. BR(Z \to qq^-). BR(Z \to invrsible) \text{ for } qqvv.$$

$$N = \sigma_{SM}. L_{int}. BR(Z \to l^+l^-). BR(Z \to qq^-) \text{ for } l^+l^-qq.$$

$$N = \sigma_{SM}. L_{int} BR. (Z \to l^+l^-). BR(Z \to l^+l^-) \text{ for } l^+l^-l^+l^-$$

where BR (Z→ ll)= 20% , BR ($Z \to qq$)=69.9% , BR ($Z \to invisible$)= 20 % (80). L_{int} =3 ab^{-1}, 15 ab^{-1} and 30 ab^{-1} for HL-LHC, HE-LHC and FCC-hh, respectively.

These four different signatures of ZZ production have some advantages over each other: while the ZZ→ $l^+l^-l^+l^-$mode is almost background-independent, if one of the two Z-bosons decays into neutrinos, it has a larger branching fraction, although there are several potentially important background processes. Besides these two decay modes, decay modes in which one of the two Z bosons decays hadronically have much larger branching fractions than the ZZ→ $l^+l^-l^+l^-$ and ZZ→ l^+l^-vv channels, but also have much higher backgrounds. Therefore, we apply χ^2 criterion to obtain 95% Confidence Level (C.L.) limits four different signatures of ZZ production on each coupling for each collider project which is considered in this thesis. The limits are discussed the following subsections where one of the Z bosons decays to vv while the other decays to e^+e^- or $\mu^+\mu^-$or qq for each collider option in thesis.

5.4.1 $llvv$ Final State

In this section we present χ^2 as a function of the different anomalous triple gauge couplings for the l^+l^-vv channel in ZZ production process for each collider option considered in thesis. In Figure 5.17. we plot χ^2 as a function of (a) f_4^{γ}, (b) f_4^{Z} , (c) f_5^{γ} , and (d) f_5^{Z} for HL-LHC with an integrated luminosity 3 ab^{-1}. In this figure, red line shows 95% C.L. limits. Similar Figures are given in Figure 5.18 and Figure 5.19 for HE-LHC and FCC-hh with are integrated luminosity 15 ab^{-1} and 30 ab^{-1}, respectively.

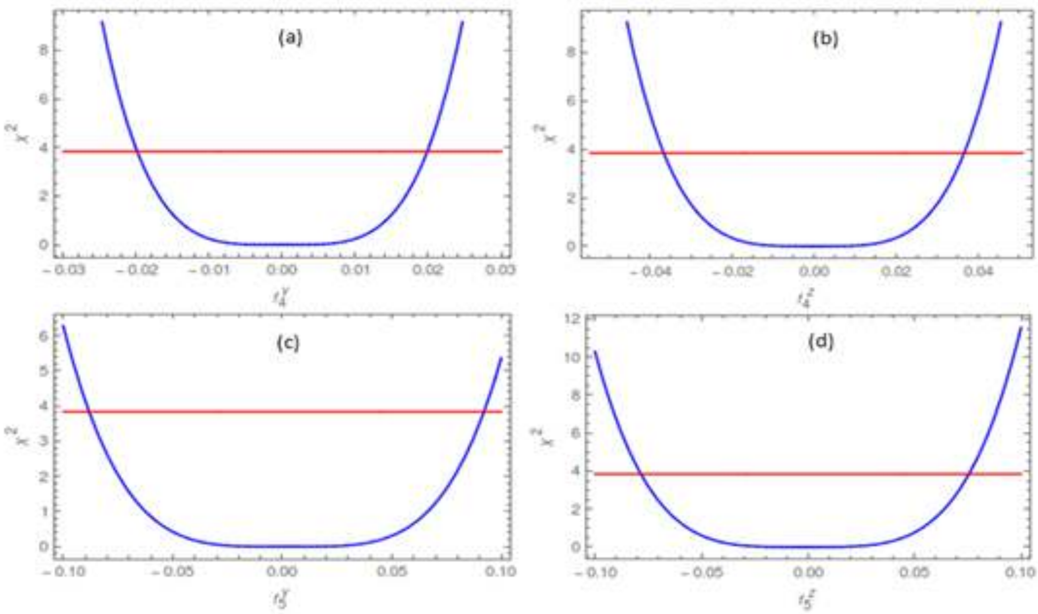

Figure 5.17. χ^2 as a function of (a) f_4^{γ}, (b) f_4^{Z}, (c) f_5^{γ} , (d) f_5^{Z} for $llvv$ channel at HL-LHC with L_{int} = 3 ab^{-1}.

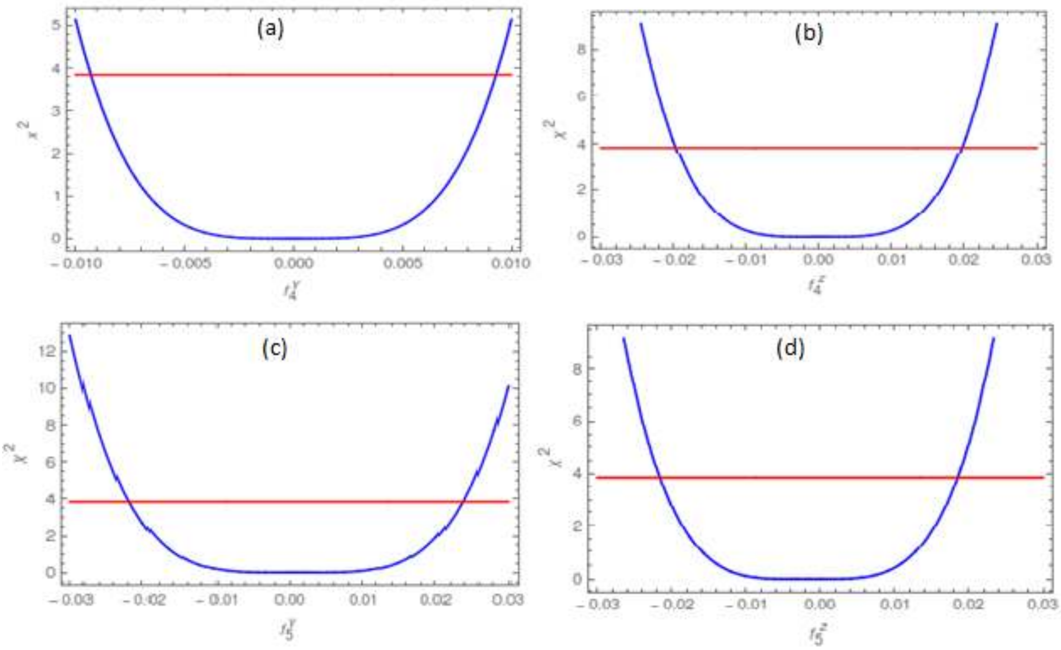

Figure 5.18. χ^2 as a function of (a) f_4^{γ}, (b) f_4^{Z}, (c) f_5^{γ}, (d) f_5^{Z} for $ll\nu\nu$ channel at HE-LHC for $\sqrt{s}$ =27 TeV with L_{int} = 15 ab^{-1}.

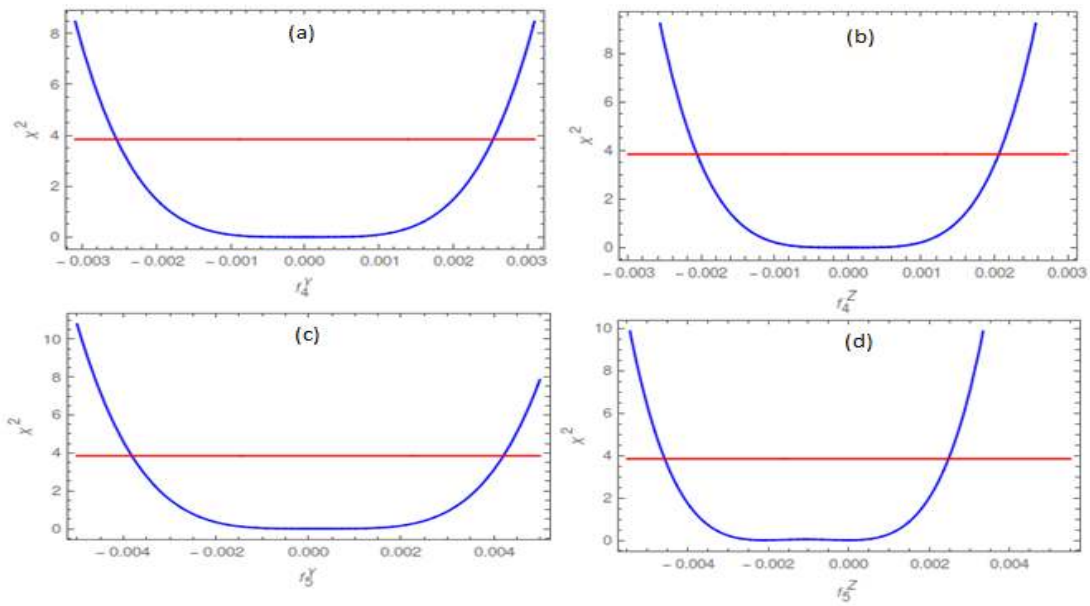

Figure 5.19. χ^2 as a function of (a) f_4^{γ}, (b) f_4^{Z}, (c) f_5^{γ}, (d) f_5^{Z} for $ll\nu\nu$ channel at FCC-hh for $\sqrt{s}$ =100 TeV with L_{int} = 30 ab^{-1}.

5.4.2 $qqvv$ Final State

In this subsection, we show χ^2 as a function of the different anomalous gauge couplings in ZZ production process with one of the Z decays to neutrons, the other two jets where the calculations correspond to the same set of colliders taken in the previous sections. Figure 5.20 shows χ^2 as a function of (a) f_4^γ , (b) f_4^Z , (c) f_5^γ , and (d) f_5^Z for HL-LHC with an integrated luminosity 3 ab^{-1}, where the blue line represents χ^2=3.84 for one parameter. Similar Figures for HE-LHC and FCC-hh are given in Figure 5.21 and Figure 5.22 with are integrated luminosity 15 ab^{-1} and 30 ab^{-1}, respectively.

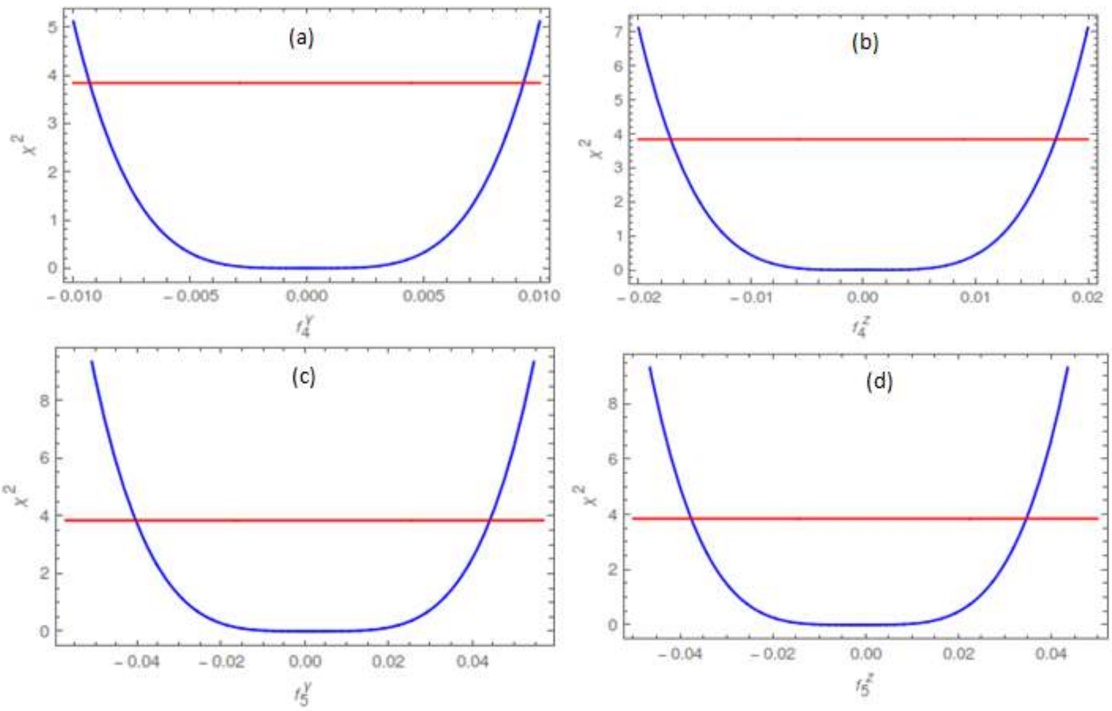

Figure 5.20. χ^2 as a function of (a) f_4^γ, (b) f_4^Z , (c) f_5^γ, (d) f_5^Z for $qqvv$ channel at HL-LHC with L_{int}= 3 ab^{-1} .

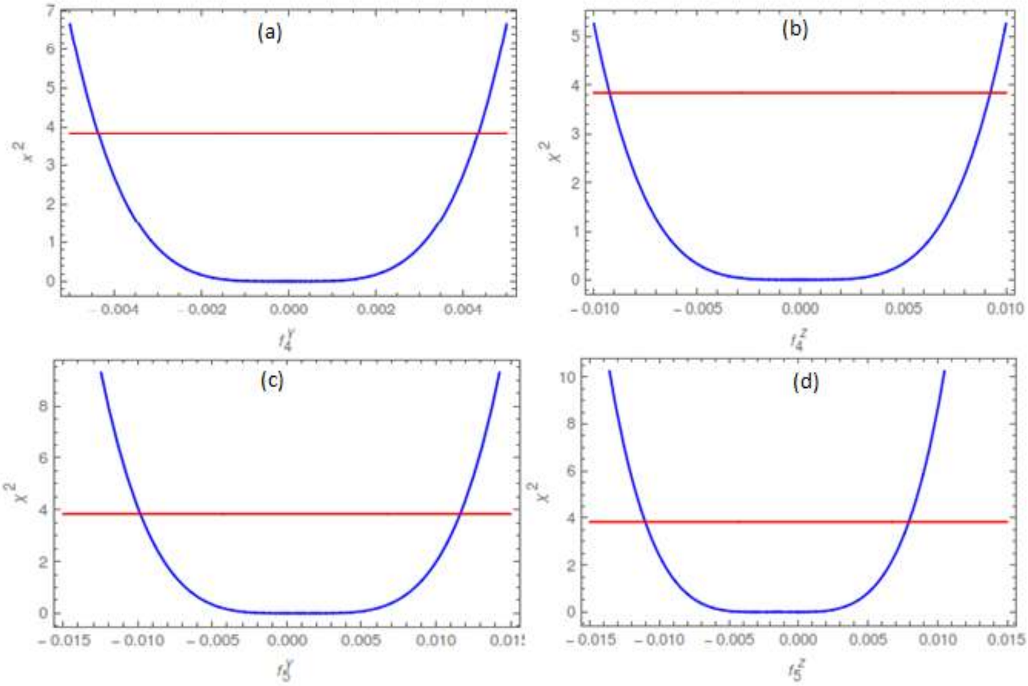

Figure 5.21. χ^2 as a function of (a) f_4^γ, (b) f_4^Z, (c) f_5^γ, (d) f_5^Z for $qqvv$ channel at HE-LHC with L_{int}= 15 ab^{-1}.

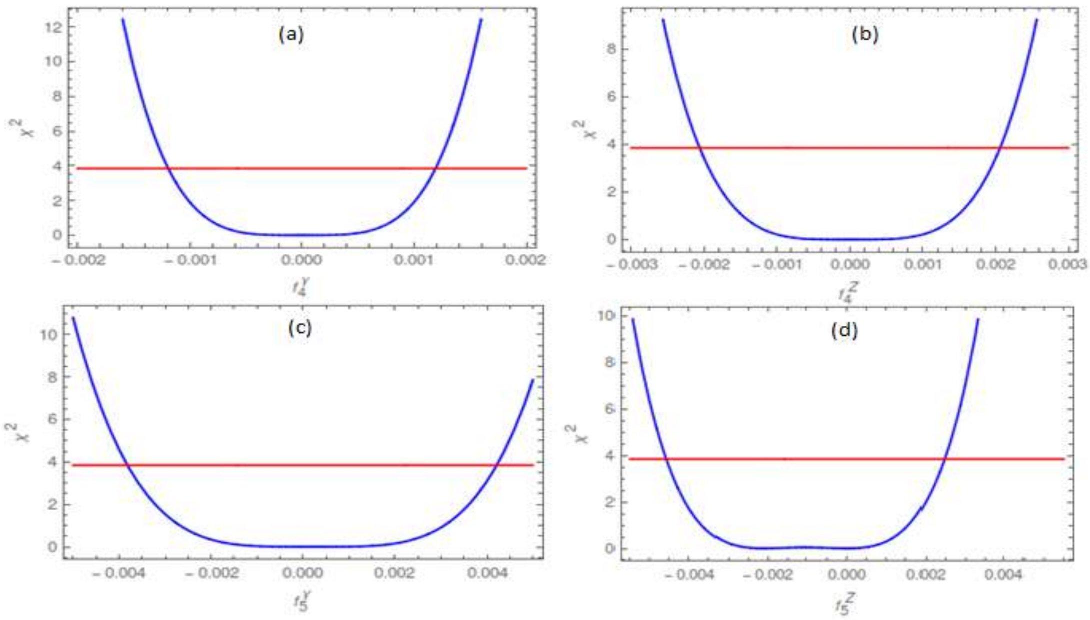

Figure 5.22. χ^2 as a function of (a) f_4^γ, (b) f_4^Z, (c) f_5^γ, and (d) f_5^Z for $qqvv$ channel at FCC-hh with L_{int} = 30 ab^{-1}.

5.4.3 l^+l^-qq Final State

In this section we display χ^2 as a function of f_4^γ, f_4^Z, f_5^γ, and f_5^Z couplings for the $llqq$ channel in ZZ production process for the same set of colliders under concern in this study. Figure 5.23 shows χ^2 as a function of (a) f_4^γ, (b) f_4^Z, (c) f_5^γ, and (d) f_5^Z for HL-LHC with an integrated luminosity 3 ab^{-1}. Similar figures for HE-LHC and FCC-hh are given in Figure 5.24 and Figure 5.25 with are integrated luminosity 15 ab^{-1} and 30 ab^{-1}, respectively.

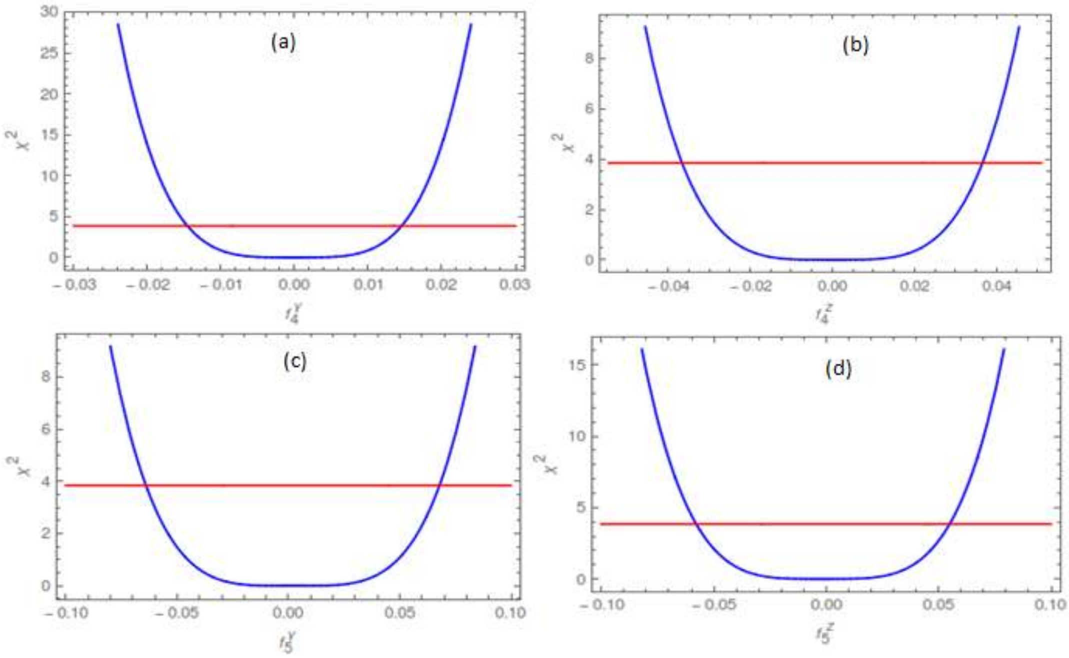

Figure 5.23. χ^2 as a function of (a) f_4^γ, (b) f_4^Z, (c) f_5^γ, (d) f_5^Z for l^+l^-qq channel at HL-LHC with L_{int} = 3 ab^{-1}.

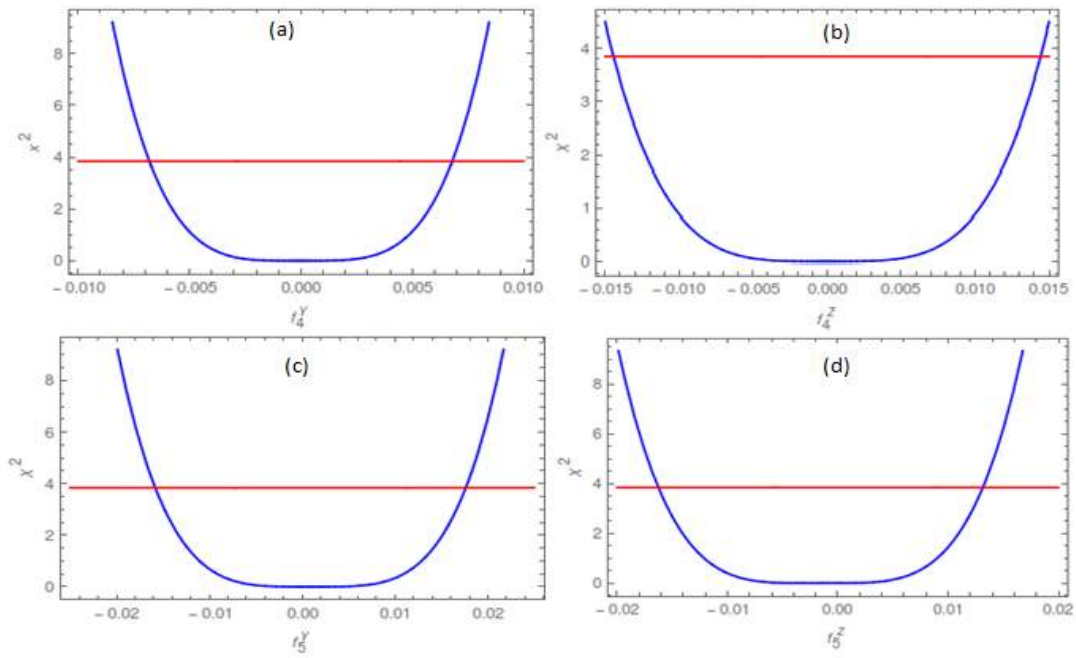

Figure 5.24. χ^2 as a function of (a) f_4^γ, (b) f_4^Z, (c) f_5^γ, and (d) f_5^Z for l^+l^-qq channel at HE-LHC with L_{int}= 15ab^{-1}.

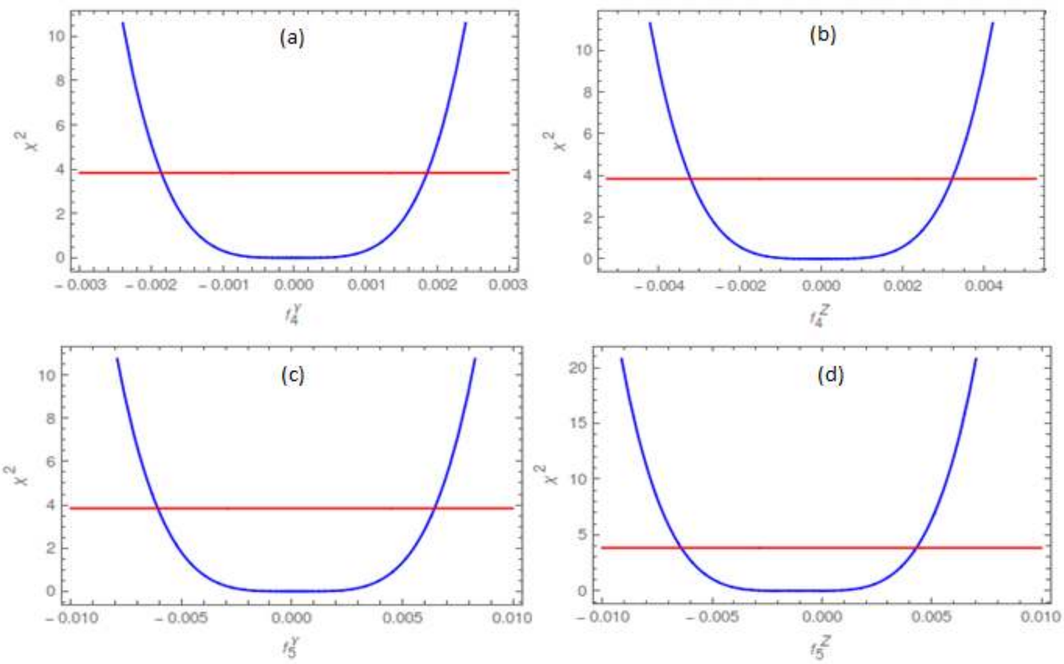

Figure 5.25. χ^2 as a function of (a) f_4^γ, (b) f_4^Z, (c) f_5^γ, (d) f_5^Z for l^+l^-qq channel at FCC-hh with L_{int} = 30 ab^{-1}.

5.4.4 $l^+l^-l^+l^-$ Final State

Considering the process $ZZ \rightarrow l^+l^-l^+l^-$ and for the same set of colliders considered before and luminosity 3ab-1 , 15ab-1 and 30ab-1 .In Figure 5.26 we plots χ^2 variation with (a) f_4^γ , (b) f_4^Z , (c) f_5^γ , and (d) f_5^Z , and similar Figures for FCC-hh and HE-LHC colliders are given in Figure 5.27 and Figure 5.28 respectively.

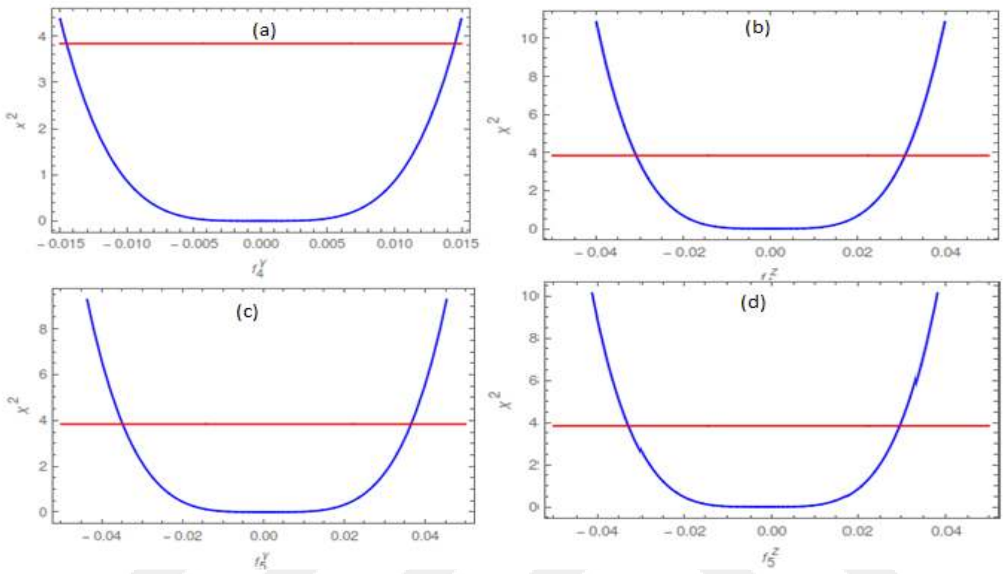

Figure 5.26. χ^2 as a function of anomalous TGC (a) f_4^γ , (b) f_4^Z , (c) f_5^γ , and (d) f_5^Z for $l^+l^-l^+l^-$ channel at HL-LHC with L_{int}= 3 ab-1.

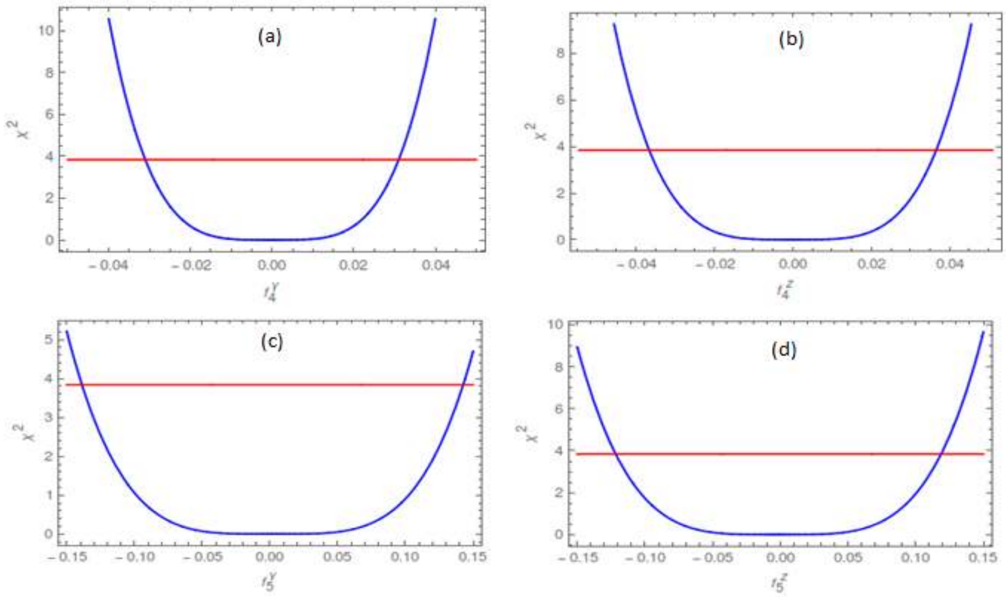

Figure 5.27. χ^2 as a function of anomalous TGC (a) f_4^γ , (b) f_4^Z , (c) f_5^γ , and (d) f_5^Z at HE-LHC with L_{int} = 15 ab-1.

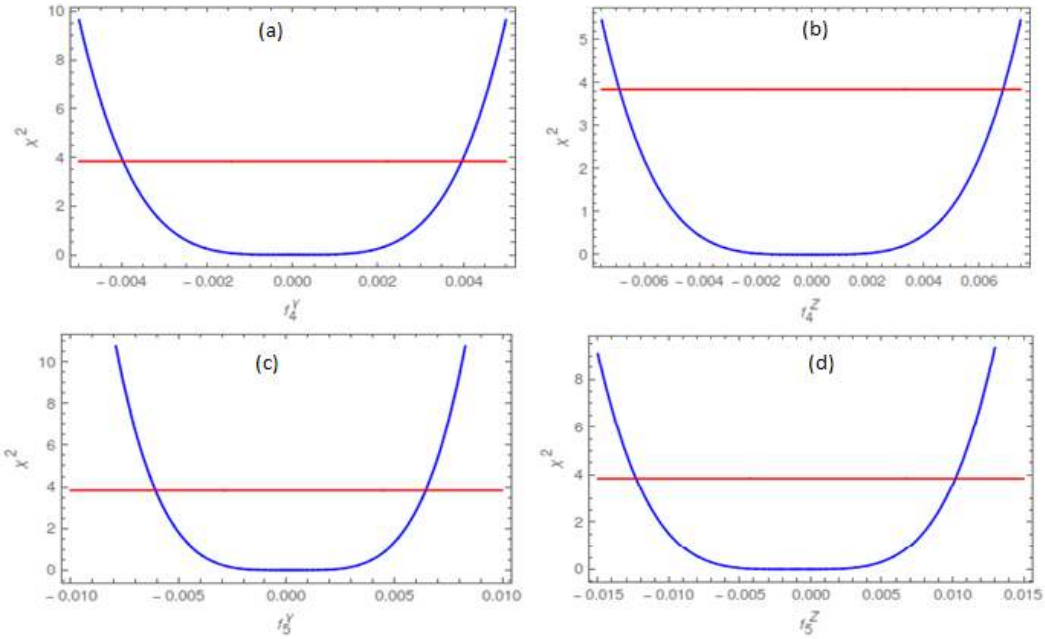

Figure 5.28. χ^2 as a function of anomalous TGC (a) f_4^γ , (b) f_4^Z , (c) f_5^γ , and (d) f_5^Z at FCC-hh with L_{int}= 30 ab^{-1}.

We turn now to the current experimental limits obtained by ATLAS and CMS collaborations for aTGCs. These limits are given in Table 5.1. The ATLAS collaborators set limits on f_4^γ, f_4^Z , f_5^γ , and f_5^Z related to the quartic ZZZ and ZZγ vertices at √s = 13 TeV and corresponding to an integrated luminosity 36.1 fb^{-1} through the measurement of ZZ production using the llνν final state (81) and four lepton final state (82). Up to date, the best limits have been obtained by CMS collaborators (83) via four-lepton final states in proton–proton collisions at a center-of-mass energy of 13 TeV with an integrated luminosity of 137fb^{-1} on the couplings f_4^γ, f_4^Z , f_5^γ ,and f_5^Z are also displayed in Table 5.1. CMS results are the most stringent limits to date on anomalous ZZZ and ZZγ triple gauge couplings and they improve the previous strictest results from ATLAS by ≈ 30–40%.

Table 5.1. Current experimental limits on anomalous $TGCs$ from ATLAS and CMS collaboration.

Couplings	$ZZ \rightarrow l^{+}l^{-}\,vv$	$ZZ \rightarrow l^{+}l^{-}l^{+}l^{-}$	
	ATLAS (81)	ATLAS (82)	CMS (83)
$f_4^{\gamma}\,x10^{-3}$	[-1.2; 1.2]	[-1.8; 1.8]	[-0.78; 0.71]
$f_4^{z}\,x10^{-3}$	[-1.0; 1.0]	[-1.5; 1.5]	[-0.66; 0.60]
$f_5^{\gamma}\,x10^{-3}$	[-1.2; 1.2]	[-1.8; 1.8]	[-0.68; 0.75]
$f_5^{z}\,x10^{-3}$	[-1.0; 1.0]	[-1.5; 1.5]	[-0.55; 0.75]

The limits values for aTGCs for four different channels of ZZ production were obtained from the values where the χ^2 distributions we obtained intersect with the 95% C.L. line. It should be noted that, we obtained the 95% C.L. limits of the aTGCs through the variation of the coefficient of one nonzero operator at a time for the set of the colliders under concern in this thesis via ZZ $\rightarrow l^{+}l^{-}vv$, , ZZ $\rightarrow qqvv$, ZZ $\rightarrow l^{+}l^{-}qq$ and ZZ $\rightarrow l^{+}l^{-}l^{+}l^{-}$process are given in Table 5.2, Table 5.3, Table 5.4 and Table 5.5, respectively. When we compared our results with ATLAS and CMS collaborations. When we made a comparison between the different Z decay channels we worked with, we obtained the best limits for f_4^{γ}, $f_4^{Z}$and f_5^{γ}couplings in the $l^{+}l^{-}qq$ channel, while for f_5^{Z} from the $qqvv$ channel from the FCC-hh collider in future colliders as you seen in Table 5.3 and Table 5.4. Our result looks one order of magnitude better compared to the current ATLAS results for all couplings, while the same order of CMS results for HE-LHC and FCC-hh.

Table 5.2. The 95% C.L. limits on $TGCs$ for process $pp \rightarrow ZZ \rightarrow l^{+}l^{-}vv$ for the set of the colliders under concern in this thesis.

Colliders	$f_4^{\gamma} x10^{-3}$	$f_4^{Z} x10^{-3}$	$f_5^{\gamma} x10^{-3}$	$f_5^{Z} x10^{-3}$
HL-LHC	[-1.98; +1.98]	[-3.65; +3.65]	[-8.82; + 9.21]	[-7.84; +7.56]
HE-LHC	[-9.29; +9.29]	[-1.97; +1.97]	[-2.19; +2.37]	[-2.15; +1.85]
FCC-hh	[-2.54; +2.54]	[-1.77; +1.48]	[-0.83; +0.87]	[-0.83; +0.62]

Table 5.3. The 95% C.L. limits on $TGCs$ for process $pp \rightarrow ZZ \rightarrow qqvv$ for the set of the colliders under concern in this thesis.

Colliders	$f_4^{\gamma} x10^{-3}$	$f_4^{Z} x10^{-3}$	$f_5^{\gamma} x10^{-3}$	$f_5^{Z} x10^{-3}$
HL-LHC	[-9.30; +9.30]	[-1.71; +1.71]	[-4.03; +4.42]	[-3.75; +3.46]
HE-LHC	[-4.35; +4.35]	[-9.24; +9.24]	[-9.83; +1.16]	[-1.10; +0.79]
FCC-hh	[-1.19; +1.19]	[-2.06; +2.06]	[-3.81; +4.21]	[-0.45; +0.24]

Table 5.4. The 95% C.L. limits on $TGCs$ for process $pp \rightarrow ZZ \rightarrow l^{+}l^{-}qq$ for the set of the colliders under concern in this thesis.

Colliders	$f_4^{\gamma} x10^{-3}$	$f_4^{Z} x10^{-3}$	$f_5^{\gamma} x10^{-3}$	$f_5^{Z} x10^{-3}$
HL-LHC	[-1.45; +1.45]	[-2.67; +2.67]	[-6.39; +6.79]	[-5.77; +5.49]
HE-LHC	[-6.80; +6.80]	[-1.44; +1.44]	[-1.58; +1.76]	[-1.62; +1.31]
FCC-hh	[-0.18; +0.18]	[-0.32; +0.32]	[-0.60; +0.64]	[-0.64; +0.43]

Table 5.5. The 95% C.L. limits on $TGCs$ for process $pp \rightarrow ZZ \rightarrow l^{+}l^{-}l^{+}l^{-}$ for the set of the colliders under concern in this thesis.

Colliders	$f_4^{\gamma} x10^{-3}$	$f_4^{Z} x10^{-3}$	$f_5^{\gamma} x10^{-3}$	$f_5^{Z} x10^{-3}$
HL-LHC	[-3.10; +3.10]	[-5.71; +5.71]	[-1.38; +1.42]	[-1.21; +1.18]
HE-LHC	[-1.45; +1.45]	[-3.08; +3.08]	[-3.47; +3.65]	[-3.27; +2.96]
FCC-hh	[-0.39; +0.39]	[-6.87; +6.87]	[-1.31; +1.35]	[-1.23; +1.02]

6. CONCLUSIONS

In these days when the installation and design of hadron-hadron colliders to come after the LHC are being discussed, researching new physics beyond the SM has gained even more importance. Accurate measurements of the self-coupling of electroweak (EW) gauge bosons play a key role in exploring new physics beyond the SM, as well as understanding the electroweak symmetry breaking mechanism. At high energies, the new physics are parametrized by an effective Lagrangian. This effective Lagrangian gives the SM one at low energy.

Since ZZ generation in hadron-hadron collisions provides an opportunity to directly investigate the self-interactions of neutral gauge bosons, we present a detailed investigation into how well it can measure ZZV couplings in future hadron-hadron colliders. In our calculations, we used the most general ZZV vertex function that takes into account Lorentz and electromagnetic gauge invariance. This vertex function defines two independent ZZZ (f_4^Z and f_5^Z) and two ZZγ (f_4^γ and f_5^γ) couplings when both Z bosons in ZZ production are assumed on the on-shell. In Chapter 2, we have given the details of these anomalous TGCs. We performed the event generation for our signal process with the CalcHEP package program, using the FCC-hh, HE-LHC and HL-LHC collider parameters, the details of which are given in chapter 3, which are planned to be established in the future.

We obtained the cross sections for the $pp \rightarrow ZZ$ process as a function of anomalous triple gauge couplings in Chapter 5. We passed the generated event files through Pythia for the hadron showering and Delphes to consider the detector effects of each collider. We have given the kinematic distributions of the final-state particles for channels $ZZ \rightarrow ll\nu\nu$, and $ZZ \rightarrow qq\nu\nu$, $ZZ \rightarrow llqq$ and $ZZ \rightarrow llll$ for each future hadron collider in chapter 5. Finally, using χ^2 test, we obtained limits for each of the hadron-hadron colliders for the four different generation channels for the f_4^Z , f_5^Z, f_4^γ and f_5^γ couplings at 95% C.L. We have obtained FCC-hh collider has the highest center of mass energy in contrast to other colliders and the best channel is $ZZ \rightarrow llqq$ for coupling f_4^γ, f_4^Z and f_5^γ but f_5^Z is $ZZ \rightarrow qq\nu\nu$.

REFERENCES

Vancouver citation system was used in this thesis.

1. Neubauer, Mark S. Diboson Production at Colliders. Annu. Rev. Nucl. Part. Sci. 2011 July. 61:223–50.

2. Hsu SC. Measurement of the ZZ production cross section and limits on anomalous neutral triple gauge couplings in proton-proton collisions at sqrt {s}= 7 TeV with the ATLAS detector. arXiv preprint arXiv:1109.6670. 2011 Sep 29.

3. Azatov A, Barducci D, Venturini E. Precision diboson measurements at hadron colliders. Journal of High Energy Physics. 2019 Apr;2019(4):1-25.

4. The ATLAS collaboration., Aaboud, M., Aad, G. et al. Measurement of the $Z\gamma\rightarrow\nu\bar{\nu}\gamma$ production cross section in pp collisions at $\sqrt{s}=13$ TeV with the ATLAS detector and limits on anomalous triple gauge-boson couplings. Journal of High Energy Physics [Internet]. 2018 Dec 31 [cited 20 Aug 2022];2018(2):1–42. Available from: https://doi.org/10.1007/JHEP12(2018)010

5. Protopapadaki S, Chevalier L, Formica A, and Laporte J. B-(eld sensors assessment, B-map study, sensors monitoring, Tech. Rep CERN, Geneva, Nov.

6. Griffiths D. Introduction to elementary particles. John Wiley & Sons; 2020 Dec 18.

7. Englert F, Brout R. Broken symmetry and the mass of gauge vector mesons. Physical Review Letters [Internet]. 1964 Aug 31 [cited 2022 May 1];13(9):321–3. Available from: https://journals.aps.org/prl/abstract/10.1103/PhysRevLett.13.321

8. Degrande C. A basis of dimension-eight operators for anomalous neutral triple gauge boson interactions. Journal of High Energy Physics. 2014 Feb;2014(2):1-7.

9. Hagiwara K, Peccei RD, Zeppenfeld D, Hikasa K. Probing the weak boson sector in $e^+ e^- \rightarrow W^+ W^-$. Nuclear Physics B. 1987 Jan 1;282:253-307.

10. Fritzsch H. The history of QCD. CERN Courier, Sept. 2012 Sep 27;27.

11. Wudka J. Electroweak effective lagrangians. International Journal of Modern Physics A. 1994 Jun 10;9(14):2301-61.

12. Gounaris GJ, Layssac J, Renard FM. New and standard physics contributions to anomalous Z and γ self-couplings. Physical Review D. 2000 Sep 12;62(7):073013.

13. Aad G, Abajyan T, Abbott B, Abdallah J, Abdel Khalek S, Abdelalim AA, et al. Observation of a new particle in the search for the Standard Model Higgs boson with the ATLAS detector at the LHC. Physics Letters B. 2012 Sep 17;716(1):1–29.

14. Higgs PW. Broken symmetries and the masses of gauge bosons. Physical Review Letters [Internet]. 1964 Oct 19 [cited 2022 May 1];13(16):508–9. Available from: https://journals.aps.org/prl/abstract/10.1103/PhysRevLett.13.508

15. Aibassov Y, Yemelyanova V, Alzhanuly B, Nakisbekov N. THE EQUATION OF HYPER-BEHAVIOR, WHICH INCLUDES HYPER-INFORMATION, HYPER-THINKING AND HYPER-CONSCIOUSNESS. InInternational Scientific and Practical Conference World science 2017 (Vol. 2, No. 9, pp. 54-56). ROST.

16. Wilson FL. Fermi's theory of beta decay. American Journal of Physics. 1968 Dec;36(12):1150-60.

17. Wells JC, Hung TT. Longman pronunciation dictionary. RELC Journal. 1990 Dec;21(2):95-7.

18. Lykken JD. Beyond the standard model. arXiv preprint arXiv:1005.1676. 2010 May 10.

19. Hewett JL, Takeuchi T, Thomas S. Indirect probes of new physics. arXiv preprint hep-ph/9603391. 1996 Mar 23 [Internet]. [cited 20 Mar 2003]. Available from: https://doi.org/10.48550/arXiv.hep-ph/9603391

20. Morrissey DE, Plehn T, Tait TM. Physics searches at the LHC. Physics reports. 2012 May 1;515(1-2):1-13.

21. Gounaris GJ, Layssac J, Renard FM. Signatures of the anomalous Z γ and ZZ production at lepton and hadron colliders. Physical Review D. 2000 Mar 9;61(7):073013.

22. Baur U, Rainwater D. Probing neutral gauge boson self-interactions in ZZ production at hadron colliders. Physical Review D. 2000 Nov 9;62(11):113011.

23. Rahaman R, Singh RK. On the choice of beam polarization in e+e−→ZZ/Zγ and anomalous triple gauge-boson couplings. The European Physical Journal C. 2017 Aug;77(8):1-9.

24. Green DR, Meade P, Pleier MA. Multiboson interactions at the LHC. Reviews of Modern Physics. 2017 Sep 20;89(3):035008.

25. Degrande C, Greiner N, Kilian W, Mattelaer O, Mebane H, Stelzer T, Willenbrock S, Zhang C. Effective field theory: a modern approach to anomalous couplings. Annals of Physics. 2013 Aug 1;335:21-32.

26. Protopapadaki ES. ZZ di-boson measurements with the ATLAS detector at the LHC and study of the toroidal magnetic fiel8d sensors. Universite de Paris XI; 2014.

27. Nardi E. Z′, new fermions, and flavor-changing processes: Constraints on E 6 models from μ→ eee. Physical Review D. 1993 Aug 1;48(3):1240.

28. Haber HE, Kane GL, Sterling T. The fermion mass scale and possible effects of Higgs bosons on experimental observables. Nuclear Physics B. 1979 Dec 17;161(2-3):493-532.

29. Abbott LF, Sikivie P, Wise MB. Constraints on charged-Higgs-boson couplings. Physical Review D. 1980 Mar 1;21(5):1393.

30. Ma E. Verifiable radiative seesaw mechanism of neutrino mass and dark matter. Physical Review D. 2006 Apr 14;73(7):077301.

31. Masip M, Pomarol A. Effects of standard model Kaluza-Klein excitations on electroweak observables. Physical Review D. 1999 Oct 8;60(9):096005.

32. Nilles HP. Supersymmetry, supergravity and particle physics. Physics Reports. 1984 Aug 1;110(1-2):1-62.

33. Martin SP. A supersymmetry primer. InPerspectives on supersymmetry II 2010 (pp. 1-153).

34. Chatrchyan S, Khachatryan V, Sirunyan AM, Tumasyan A, Adam W, Aguilo E, et al. Observation of a new boson at a mass of 125 GeV with the CMS experiment at the LHC. Physics Letters B. 2012 Sep 17; 716(1):30–61.

35. Glashow SL. Partial-symmetries of weak interactions. Nuclear physics. 1961 Feb 1;22(4):579-88.

36. Englert F, Brout R. Broken symmetry and the mass of gauge vector mesons. Physical review letters. 1964 Aug 31;13(9):321.

37. Campbell JM, Ellis RK, Williams C. Vector boson pair production at the LHC. Journal of High Energy Physics. 2011 Jul;2011(7):1-36.

38. ATLAS collaboration. Luminosity determination in pp collisions at root (s) = 7 TeV using the ATLAS detector at the LHC. European Physical Journal C: Particles and Fields. 2011;71(4).

39. ATLAS Muon Collaboration. Atlas muon spectrometer technical design report. CERN/LHCC. 1997 Jun:97-22.

40. ATLAS Muon Collaboration. Atlas muon spectrometer technical design report. CERN/LHCC. 1997 Dec 15:97-32.

41. Sanfilippo S. Hall probes: physics and application to magnetometry. CERN Accelerator School Magnets. 2010 Nov 30:423.

42. Unal G, Froidevaux D. Higgs mass measurements and uncertainties in 2011 and 2012 data. Tech. rep. ATL-COM-PHYS-2012-1774. Geneva: CERN; 2012 Dec.

43. Council CE. European strategy session of Council. CERN-Council-S/106 (May 30, 2013). 2013.

44. Brüning O, Rossi L, editors. The High Luminosity Large Hadron Collider: the new machine for illuminating the mysteries of Universe. World Scientific Publishing Company; 2015 Aug 28.

45. Apollinari G, Brüning O, Nakamoto T, Rossi L. High-Luminosity Large Hadron Collider. Technical Design Report CERN-2015. 2015 Dec;5.

46. Apollinari G, Brüning O, Nakamoto T, Rossi L. High luminosity large hadron collider HL-LHC. arXiv preprint arXiv:1705.08830. 2017 May 24.

47. Selvaggi M. Higgs measurements at FCC-hh. CERN Notes [Internet]. [cited 2018 Apr 28]. Available from: https://cds. cern. ch/record/2642471

48. Benedikt M, Zimmermann F. Future Circular Collider (FCC) Study. InFuture Circular Collider Study Kickoff Meeting, University of Geneva, Geneva, Switzerland 2014 Feb.

49. Abelleira JL. Flat-beam IR optics. InJoint Snowmass-EUCARD/AccNet-HiLumi LHC meeting.'Frontier capabilities for Hadron colliders' 2013 (No. POST_TALK).

50. Benedikt M. Future circular collider study. FCC-DRAFT-MGMT-2016-008; 2014 May 22.

51. Zimmermann F, Benedikt M, Garrido MC, Cerutti F, Goddard B, Gutleber J, Jimenez JM, Mangano M, Mertens V, Osborne JA, Otto T. Future circular collider. CERN-ACC-2018-0059; 2018 Dec.

52. Helsens C, Selvaggi M. Search for high-mass resonances at FCC-hh. FCC-DRAFT-PHYS-2018-004; 2018 Oct 9.

53. Ferrenberg AM, Swendsen RH. Optimized monte carlo data analysis. Computers in Physics. 1989 Sep 1 [Internet]. [cited 04 Jun 1998]; 3(5):101-4 Available from: https://doi.org/10.1063/1.4822862

54. Pukhov A, Boos E, Dubinin M, Edneral V, Ilyin V, Kovalenko D, Kryukov A, Savrin V, Shichanin S, Semenov A. CompHEP-a package for evaluation of Feynman diagrams and integration over multi-particle phase space. User's manual for version 33. arXiv preprint hep-ph/9908288. 1999 Aug 6.

55. Küblbeck J, Böhm M, Denner A. Feyn Arts—computer-algebraic generation of Feynman graphs and amplitudes. Computer Physics Communications. 1990 Sep 1;60(2):165-80. *63

56. Ishikawa T, Kaneko T, Kato K, Kawabata S, Shimizu Y, Tanaka T. GRACE Manual, Version 1.0; KEK Report 92-19. Comp. Phys. Commun. 1993;92:127-52.

57. Murayama H, Watanabe I, Hagiwara K. HELAS: HELicity amplitude subroutines for Feynman diagram evaluations. National Lab. for High Energy Physics; 1992.

58. Stelzer T, Long WF. Automatic generation of tree level helicity amplitudes. Computer Physics Communications. 1994 Jul 1;81(3):357-71.

59. Papadopoulos CG. PHEGAS: a phase-space generator for automatic cross-section computation.

arXiv preprint hep-ph/0007335. 2000 Jul.

60. Moretti M, Ohl T, Reuter J. O'Mega: An Optimizing matrix element generator. arXiv preprint hep-ph/0102195. 2001 Feb 15.

61. Hahn T. Generating Feynman diagrams and amplitudes with FeynArts 3. Computer Physics Communications. 2001 Nov 1;140(3):418-31.

62. Hahn T. Automatic loop calculations with FeynArts, FormCalc, and LoopTools. Nuclear Physics B-Proceedings Supplements. 2000 Oct 1;89(1-3):231-6.

63. Maltoni F, Stelzer T. MadEvent: Automatic event generation with MadGraph. Journal of High Energy Physics. 2003 Feb 21;2003(02):027.

64. Alwall J, Herquet M, Maltoni F, Mattelaerc O, Stelzerd T. MadGraph 5: going beyond. Journal of High Energy Physics [Internet]. 2011 Jun 28 [cited 2022 Jun 7];2011(6):1–40. Available from: https://link.springer.com/article/10.1007/JHEP06(2011)128

65. Kanaki A, Papadopoulos CG. HELAC: a package to compute electroweak helicity amplitudes. Computer physics communications. 2000 Nov 1;132(3):306-15.

66. Papadopoulos CG. PHEGAS: A phase-space generator for automatic cross-section computation. Computer physics communications. 2001 Jun 15;137(2):247-54.

67. Cafarella A, Papadopoulos CG, Worek M. Helac-Phegas: a generator for all parton level processes. Computer Physics Communications. 2009 Oct 1;180(10):1941-55.

68. Kilian W, Ohl T, Reuter J. WHIZARD: Simulating Multi-Particle Processes at LHC and ILC. arXiv preprint arXiv:0708.4233. 2007 Aug 30.

69. Gleisberg T, Hoeche S, Krauss F, Schälicke A, Schumann S, Winter JC. SHERPA 1. α, a proof-of-concept version. Journal of High Energy Physics. 2004 Mar 8;2004(02):056.

70. Gleisberg T, Höche S, Krauss F, Schönherr M, Schumann S, Siegert F, Winter J. Event generation with SHERPA 1.1. Journal of High Energy Physics. 2009 Feb 3;2009(02):007.

71. Pukhov A. CalcHEP 2.3: MSSM, structure functions, event generation, batchs, and generation of matrix elements for other packages. arXiv preprint hep-ph/0412191. 2004 Dec 14.

72. KONG K. TASI 2011: CalcHEP and PYTHIA Tutorials. Dark Secrets Of The Terascale, The (Tasi 2011)–Proceedings Of The 2011 Theoretical Advanced Study Institute In Elementary Particle Physics. 2012 Dec 31:161.

73. Belyaev A, Christensen ND, Pukhov A. CalcHEP 3.4 for collider physics within and beyond the Standard Model. Computer Physics Communications. 2013 Jul 1;184(7):1729-69.

74. Kong K. TASI 2011: CalcHEP and PYTHIA Tutorials. arXiv preprint arXiv:1208.0035. 2012 Jul 31.

75. Pumplin J, Stump DR, Huston J, Lai HL, Nadolsky P, Tung WK. New generation of parton distributions with uncertainties from global QCD analysis. Journal of High Energy Physics. 2002 Aug 9;2002(07):012.

76. Sjöstrand T, Ask S, Christiansen JR, Corke R, Desai N, Ilten P, Mrenna S, Prestel S, Rasmussen CO, Skands PZ. An introduction to PYTHIA 8.2. Computer physics communications. 2015 Jun 1;191:159-77.

77. De Favereau J, Delaere C, Demin P, Giammanco A, Lemaitre V, Mertens A, Selvaggi M. DELPHES 3: a modular framework for fast simulation of a generic collider experiment. Journal of High Energy Physics. 2014 Feb;2014(2):1-26.

78. "ExROOT Analysis [Internet]. [cited 2022 Agust 28]. Available from: http://madgraph.hep.uiuc.edu/Downloads/ExRootAnalysis

79. Mary L. McHugh. The Chi-square test of independence. Biochem Med (Zagreb). 2013 Jun; 23(2): 143–149.

80. Tanabashi. M. et al. The 2018 edition of the Review of Particle Physics. Physical Review D. 2018 Aug 17; 98: 030001.

81. The ATLAS collaboration., Aaboud, M., Aad, G. et al. Measurement of the $Z\gamma \rightarrow \nu\overline{\nu}\gamma$ production cross section in pp collisions at $\sqrt{s}=13$ TeV with the ATLAS detector and limits on anomalous triple gauge-boson couplings. Journal of High Energy Physics [Internet]. 2018 Dec 31 [cited 20 Aug 2022];2018(2):1–42. Available from: https://doi.org/10.1007/JHEP12(2018)010.

82. ATLAS., Aaboud M, Aad G, Abbott B, Abeloos B, Abidi SH, AbouZeid OS, Abraham NL, Abramowicz H, Abreu H, Abreu R, Abulaiti Y. $ZZ \rightarrow \ell^+ \ell^- \ell'^+ \ell'^-$ cross-section measurements and search for anomalous triple gauge couplings in 13 TeV p p collisions with the ATLAS detector. Physical Review D. 2018 Feb 7;97(3):032005.

83. Sirunyan, A.M., Tumasyan, A., Adam, W. et al. Measurements of $pp \rightarrow ZZ$ production cross sections and constraints on anomalous triple gauge couplings at $\sqrt{s}=13$TeV. Eur. Phys. The European Physical Journal C - Particles and Fields [Internet]. 2021 Mar 1. [cited 2021 Mar 1];81(200). Available from: https://doi.org/10.1140/epjc/s10052-020-08817-8